THE JOURNAL OF BIOLOGICAL CHEMISTRY Vol. 276, No. 52, Issue of December 28, pp. 48679–48692, 2001
Printed in U.S.A.

Hyaluronan Promotes CD44v3-Vav2 Interaction with Grb2-p185^{HER2} and Induces Rac1 and Ras Signaling during Ovarian Tumor Cell Migration and Growth*

Received for publication, July 18, 2001, and in revised form, October 15, 2001
Published, JBC Papers in Press, October 17, 2001, DOI 10.1074/jbc.M106759200

Lilly Y. W. Bourguignon‡§, Hongbo Zhu‡, Bo Zhou‡, Falko Diedrich‡¶, Patrick A. Singleton‖, and Mien-Chie Hung‡‡**

From the ‡Department of Medicine, University of California and Endocrine Unit, Veterans Affairs Medical Center, San Francisco, California 94121, the ‖Department of Cell Biology and Anatomy, University of Miami School of Medicine, Miami, Florida 33101, and the ‡‡Department of Molecular and Cellular Oncology, the University of Texas M. D. Anderson Cancer Center, Houston, Texas 77030

In this study we initially examined the interaction between CD44v3 (a hyaluronan (HA) receptor) and Vav2 (a guanine nucleotide exchange factor) in human ovarian tumor cells (SK-OV-3.ipl cell line). Immunological data indicate that both CD44v3 and Vav2 are expressed in SK-OV-3.ipl cells and that these two proteins are physically linked as a complex *in vivo*. By using recombinant fragments of Vav2 and *in vitro* binding assays, we have detected a specific binding interaction between the SH3-SH2-SH3 domain of Vav2 and the cytoplasmic domain of CD44. In addition, we have observed that the binding of HA to CD44v3 activates Vav2-mediated Rac1 signaling leading to ovarian tumor cell migration. Further analyses indicate that the adaptor molecule, growth factor receptor-bound protein 2 (Grb2) that is bound to p185^{HER2} (an oncogene product), is also associated with the CD44v3-Vav2 complex. HA binding to SK-OV-3.ipl cells promotes recruitment of both Grb2 and p185^{HER2} to the CD44v3-Vav2 complex leading to Ras activation and ovarian tumor cell growth. In order to determine the role of Grb2 in CD44v3 signaling, we have transfected SK-OV-3.ipl cells with Grb2 mutant cDNAs (*e.g.* ΔN-Grb2 that has a deletion in the amino-terminal SH3 domain or ΔC-Grb2 that has a deletion in the carboxyl-terminal SH3 domain). Our results clearly indicate that the SH3 domain deletion mutants of Grb2 (*i.e.* the ΔN-Grb2 (and to a lesser extent the ΔC-Grb2) mutant) not only block their association with p185^{HER2} but also significantly impair their binding to the CD44v3-Vav2 complex and inhibit HA/CD44v3-induced ovarian tumor cell behaviors. Taken together, these findings strongly suggest that the interaction of CD44v3-Vav2 with Grb2-p185^{HER2} plays an important role in the coactivation of both Rac1 and Ras signaling that is required for HA-mediated human ovarian tumor progression.

The cell adhesion molecule, CD44, is a product of a single gene that undergoes alternative splicing of 12 possible exons to generate variant isoforms (1). Nucleotide sequence analyses reveal that the CD44 isoforms are variants of the standard form, CD44s (1). CD44s (molecular mass ≈85 kDa) is the most common isoform of CD44 found in many cell types including human ovarian carcinoma cells (2). CD44 can be further modified by extensive *N*- and *O*-glycosylations and glycosaminoglycan additions (3–5). Apparently, both post-translational modifications and/or alternative splicing within the CD44 structure determine the functional outcome of this molecule. CD44 is a transmembrane glycoprotein that is one of the major hyaluronan (HA)[1] receptors (6). CD44 binds to extracellular matrix components (*i.e.* HA) at its amino terminus of the extracellular domain (7, 8). CD44 also contains specific binding sites for the cytoskeleton (9–14) and various signaling molecules (15–19) within the 70-amino acid carboxyl terminus in the cytoplasmic domain.

Both CD44 and HA appear to be overexpressed at sites of tumor attachment and are known to be involved in cell aggregation, proliferation, migration, and angiogenesis (15–23). Specifically, HA is present in large amounts in the mesothelial lining of the peritoneum (24). In fact, it has been postulated that CD44 interaction with HA may be one of the important requirements for the peritoneal spread of ovarian cancer. However, the cellular and molecular mechanisms controlling the ability of CD44-positive ovarian tumor cells to migrate and implant at HA-enriched locations within the peritoneal cavity remain poorly understood, and the oncogenic mechanism(s) required for HA-activated and CD44-specific ovarian tumor progression remain(s) to be determined.

Several lines of evidence indicate that the binding of HA to CD44 promotes Rac1 signaling and tumor cell activation (17, 18). A recent paper (17) reports that the interaction between CD44v3 isoform and Tiam1, one of the guanine nucleotide exchange factors (GEFs, the Dbl or DH family), up-regulates Rac1 signaling and cytoskeleton-mediated metastatic breast tumor progression. To date, at least 30 different GEFs have been identified (25, 26). In the search for other CD44 isoform-linked GEFs, which correlate with metastatic behavior, a prime candidate, named Vav2,

* This work was supported in part by United States Public Health Grants CA66163 and CA 78633, Department of Defense Grants DAMD 17-97-1-7014 and DAMD 17-99-1-9291, and the generous donation from the late Dennece Mason. The costs of publication of this article were defrayed in part by the payment of page charges. This article must therefore be hereby marked "*advertisement*" in accordance with 18 U.S.C. Section 1734 solely to indicate this fact.

§ To whom correspondence should be addressed: Endocrine Unit (111N), Dept. of Medicine, University of California San Francisco, and Veterans Affairs Medical Center, 4150 Clement St., San Francisco, CA 94121. Tel.: 415-221-4810 (Ext. 3321); Fax: 415-750-6929; E-mail: lillyb@itsa.ucsf.edu.

¶ Supported by a research fellowship from the Deutsche Forschungsgemeinschaft.

** Supported by American Heart Association predoctoral fellowship.

[1] The abbreviations used are: HA, hyaluronan; PBS, phosphate-buffered saline; GEFs, guanine nucleotide exchange factor(s); DH, Dbl homology; PH, pleckstrin homology; RT, reverse transcription; GTPγS, guanosine 5′-3-*O*-(thio)triphosphate; AMP-PNP, adenyl-5′-yl β,γ-imidodiphosphate; GST, glutathione *S*-transferase; aa, amino acids; MAPK, mitogen-activated protein kinase; MEK, mitogen-activated protein kinase/extracellular signal-regulated kinase kinase; SH, Src homology.

has been identified. Vav2 is a member of the Vav family of oncoproteins known to act as a GEF for RhoGTPases (*e.g.* Rac1, RhoA, and Cdc42) in a phosphotyrosine-dependent manner (27). The Vav molecule was first identified as an oncogene based on its ability to induce cell transformation following gene transfer using human tumor DNA (28). Vav1 is expressed exclusively in hematopoietic cells, whereas the homologous protein, Vav2, is now known to be expressed ubiquitously (29, 30). Structurally, Vav2 is a 95–100-kDa protein, which contains numerous functional domains and structural motifs found in signal transduction proteins and oncoproteins. These motifs include amino-terminal calponin homology/leucine-rich and acid-rich domains (31), a Dbl homology domain (DH) (32, 33), a pleckstrin homology domain (PH) (34), a cysteine-rich zinc-binding domain (CR) (31), and two src homology-3 (SH3) domains flanking a single SH2 domain (35, 36). In particular, the sequence between aa 198 and 469 contains significant sequence homology to the DH of many proteins, which exhibit GDP/GTP exchange activity for specific members of the Ras superfamily of GTP-binding proteins (32, 33). *In vitro*, Vav2 has been clearly shown to act as a GDP/GTP exchange protein for the Rho subfamily of GTPases, including Rac1, Cdc42, RhoA, RhoB, and RhoG (27, 37–40). In addition, Vav2 contains one pleckstrin homology domain (PH), which is commonly detected in signaling molecules and cytoskeletal proteins (41, 42). The PH domain may also mediate the association of Vav2 with the submembrane region of the cell via protein-protein or protein-lipid interactions (41, 42). The carboxyl-terminal region of Vav2 contains an SH2 domain surrounded by two SH3 domains. Although its function is still unclear, this region may facilitate interactions with submembrane signaling complexes.

It has been shown that overexpression of Vav2 is sufficient to activate its oncogenic potential (30). Vav2-induced cytoskeletal changes and cellular transformation are comparable, but not identical, to those induced by other members of the Dbl family of oncoproteins (30). Taken together, these sequence analyses of Vav2 suggest that Vav2 association with the transforming phenotype may be mediated via submembrane cytoskeletal regulation and/or activation of Rho family GTPases. Activation of Rac1, Cdc42, and RhoA has been shown to produce specific structural changes in the plasma membrane associated with cell movement such as lamellipodia, filopodia, and stress fiber formation, respectively (43). The coordinated activation of these GTPases is considered to be a possible mechanism underlying tumor cell motility and migration, an obvious prerequisite for metastasis (9–11).

The HER2 oncogene (also called c-ErbB-2 or Neu) encodes an 185-kDa ($p185^{HER2}$) membrane protein, which contains a single transmembrane spanning region, two cystine-rich extracellular domains, and a tyrosine kinase-associated cytoplasmic domain (44). This protein belongs to the epidermal growth factor receptor subgroup of the receptor-linked tyrosine kinase superfamily (45). Overexpression or amplification of HER2 oncogene appears to correlate with poor survival rates of many known cancers including ovarian cancer (46, 47). For example, the overall survival rate and time of relapse for patients with HER2 overexpression is significantly less than patients lacking HER2 overexpression (46, 47). A number of published reports (46–48) have demonstrated that HER2 overexpression is a causative factor (and not a consequence) of human cancer. Previous studies in transformed cells have also shown that guanidine nucleotide (GDP/GTP) exchange on Ras is stimulated by tyrosine phosphorylation of $p185^{HER2}$ and recruitment of the Sos exchange factor to the plasma membrane with the aid of the Grb2 adaptor protein (48–54). In addition, dominant-negative mutants of Grb2 induced reversal of the transformed phenotype caused by point mutation-activated Rat HER-2/Neu (55). It appears that activation of $p185^{HER2}$ tyrosine kinase leads to Ras-mediated stimulation of a downstream kinase cascade, which at least includes Raf-1/MEK/MAPK and MEKK-1/JNKK/JNK pathways leading to cell growth (48–55). Previously, we have determined that CD44 and $p185^{HER2}$ are physically linked to each other via interchain disulfide bonds in human ovarian tumor cells (SK-OV-3.ipl cell line) (2). Most importantly, HA binding to a CD44-associated $p185^{HER2}$ complex activates the $p185^{HER2}$ tyrosine kinase activity and promotes ovarian carcinoma cell growth (2). We believe that direct "cross-talk" between the two surface molecules, CD44 and the $p185^{HER2}$, may be one of the most important signaling events in human ovarian carcinoma development.

In this study we have investigated a CD44v3-Vav2 interaction with Grb2-linked $p185^{HER2}$ in ovarian tumor cells in order to understand further the fundamental nature of tumorigenesis and metastasis in this lethal gynecological malignancy. By using a variety of biochemical and molecular biological techniques, we have found that both CD44v3 and Vav2 are overexpressed in human ovarian tumor cells (*e.g.* SK-OV-3.ipl cell line) and that CD44v3 is closely associated with Vav2 (in particular, the SH3-SH2-SH3 domain of Vav2) in SK-OV-3.ipl cells. Most importantly, we have established that the binding of HA to SK-OV-3.ipl cells stimulates CD44v3-specific Rac1 and Ras signaling and association of the linker molecule, Grb2, with CD44v3-Vav2 and $p185^{HER2}$ leading to ovarian tumor cell migration and growth. Furthermore, transfection of SK-OV-3.ipl cells with Grb2 mutant cDNAs (ΔN-Grb2cDNA and to a lesser extent the ΔC-Grb2cDNA) significantly inhibits Grb2 association with CD44v3-Vav2 and $p185^{HER2}$. Further analyses indicate that overexpression of the ΔN-Grb2 mutant (and to a lesser extent the ΔC-Grb2) not only significantly impairs both Rac1 and Ras signaling but also inhibits ovarian tumor cell migration and growth. These findings suggest that CD44v3-Vav2 interactions with Grb2-linked $p185^{HER2}$ are involved in the stimulation of both Rac1 and Ras signaling leading to the concomitant activation of HA-mediated ovarian tumor cell migration and growth.

MATERIALS AND METHODS

Cell Culture—The SK-OV-3.ipl cell line was established from ascites that developed in a nu/nu mouse given an intraperitoneal injection of SK-OV-3 human ovarian carcinoma cell line (obtained from the American Type Culture Collection) as described previously (56). Cells were grown in Dulbecco's modified Eagle's medium/F-12 medium (Life Technologies, Inc.) supplemented with 10% fetal bovine serum. Cells were routinely serum-starved (and therefore deprived of serum HA) before adding HA.

COS-7 cells were obtained from American Type Culture Collection and grown routinely in Dulbecco's modified Eagle's medium containing 10% fetal bovine serum, 1% glutamine, 1% penicillin, and 1% streptomycin.

Antibodies and Various Reagents—Monoclonal rat anti-CD44 antibody (clone, 020; isotype, IgG_{2b}; obtained from CMB-TECH, Inc., San Francisco, CA) used in this study recognizes a common determinant of the CD44 class of glycoproteins, including CD44v3 isoform (15, 17, 56). For the preparation of polyclonal rabbit anti-CD44v3 or rabbit anti-Vav2, specific synthetic peptides (≈15–17 amino acids unique for either CD44v3 sequences or Vav2 sequences) were prepared, respectively, by the Peptide Laboratories of Department of Biochemistry and Molecular Biology using an Advanced Chemtech automatic synthesizer (model ACT350). Conjugated CD44v3 or Vav2 (to hemocyanin or polylysine) was injected into rabbits (or rat) to raise the antibodies. The anti-CD44v3 or anti-Vav2 sera were collected from each bleed and stored at 4 °C containing 0.1% azide. Both rabbit anti-CD44v3 and rabbit anti-Vav2 IgGs were prepared using conventional DEAE-cellulose chromatography and were tested to be monospecific (by immunoblot assays). Monoclonal mouse anti-$p185^{HER2}$ antibody (c-neu-ab-3) and rat anti-Ras antibody (Y13-259) were purchased from Oncogene Science, Inc. Monoclonal mouse anti-Grb2 antibody was from Transduction Labora-

tories. Monoclonal mouse anti-HA1 (hemagglutinin epitope) antibody (clone 12 CA5) and mouse anti-Xpress™ were obtained from Roche Molecular Biochemicals and Invitrogen, respectively. Both rooster comb H and fibronectin were purchased from Sigma. A highly polymerized form (~10^6 daltons) of HA was purified by gel filtration column chromatography using Sephacryl S1000 column as described previously (5).

Reverse Transcriptase-PCR and One-step Cloning—Total RNA was extracted from SK-OV-3.ipl cells using the acid guanidinium thiocyanate-phenol-chloroform technique as described previously (57). Approximately 3 μg of total RNA was used with an oligo(dT) primer in a reverse transcriptase system (Promega, Madison, WI) to synthesize cDNA at 42 °C for 1 h, using avian myeloblastosis virus-reverse transcriptase. After synthesis of the first strand, PCR of the CD44 cDNA was done by initial melting of the RNA/cDNA at 94 °C for 4 min, then 35 cycles of denaturation at 94 °C for 30 s, annealing at 60 °C for 30 s, and polymerization at 72 °C for 1 min. The PCR primers were designed initially to look at and amplify the region involved with alternative splicing. Analysis of the presence of v3-containing isoforms was facilitated by designing PCR primers within exon 5 and v3 (exon 7). Specifically the primers were CD44 exon 5 (exon 5, 5′-GCACTTCAGGAGGTTACATC-3′) and CD44 v3(exon 7) (exon 7, 5′-CTGAGGTGTCTGTCTCTTTC-3′). The PCR products were one-step-cloned using TA cloning kit (Invitrogen, San Diego, CA) and sequenced by dideoxy sequencing method.

For the detection of Vav2 expression, ~3 μg of total RNA isolated from SK-OV-3.ipl cells was used for RT-PCR analysis using SUPERSCRIPT™ ONE-STEP RT-PCR with PLATINUM® *Taq* system (Life Technologies, Inc.). Two Vav2-specific primers (5′-GCGATGTACATCAATGAAGTTAAACG-3′ and 5′-GCCCTCCTCTTCTACGTACGTT-3′) were designed for this study. The reactions were cycled after an initial 2-min denaturation at 94 °C followed by 35 cycles of denaturation at 94 °C for 30 s, annealing at 60 °C for 30 s, and polymerization at 72 °C for 2 min. The PCR products were analyzed using a 2.0% agarose gel electrophoresis and visualized by ethidium bromide staining. As controls, RT-PCR was carried out in the absence of SUPERSCRIPT II reverse transcriptase or in the absence of template in the PCR mixture. No amplification products were detected in these control samples.

Cell Surface Labeling Procedures—SK-OV-3.ipl cells suspended in PBS were surface-labeled using the following biotinylation procedure. Briefly, cells (10^7 cells/ml) were incubated with sulfosuccinimidyl-6-(biotinamido)hexanoate (Pierce) (0.1 mg/ml) in labeling buffer (150 μM NaCl, 0.1 M HEPES (pH 8.0)) for 30 min at room temperature. Cells were then washed with PBS to remove free biotin. Subsequently, the biotinylated cells were used for anti-CD44v3-mediated immunoprecipitation as described previously (56). These biotinylated materials precipitated by anti-CD44v3 antibody were analyzed by SDS-PAGE, transferred to the nitrocellulose filters, and incubated with ExtrAvidin-peroxidase (Sigma). After an addition of peroxidase substrate (Pierce), the blots were developed using ECL chemiluminescence reagent (Amersham Biosciences) according to the manufacturer's instructions.

Immunoprecipitation and Immunoblotting Techniques—SK-OV-3.ipl cells were solubilized in 50 mM HEPES (pH 7.5), 150 mM NaCl, 20 mM $MgCl_2$, 0.5% Nonidet P-40, 0.2 mM Na_3VO_4, 0.2 mM phenylmethylsulfonyl fluoride, 10 μg/ml leupeptin, and 5 μg/ml aprotinin and immunoprecipitated using rat anti-CD44 antibody or rabbit anti-Vav2 antibody followed by goat anti-rabbit IgG, respectively. The immunoprecipitated material was solubilized in SDS sample buffer, electrophoresed, and blotted onto the nitrocellulose. After blocking nonspecific sites with 3% bovine serum albumin, the nitrocellulose filter was incubated with rabbit anti-Vav2 antibody (5 μg/ml) or rat anti-CD44 antibody/rabbit anti-CD44v3 antibody (5 μg/ml), respectively, for 1 h at room temperature followed by incubation with horseradish peroxidase-conjugated goat anti-rabbit IgG (1:10,000 dilution) at room temperature for 1 h. The blots were then developed using ECL chemiluminescence reagent (Amersham Biosciences) according to the manufacturer's instructions. SK-OV-3.ipl cells (treated with 50 μg/ml HA for 10 min or without any HA treatment) were solubilized by Nonidet P-40 (as described above) and immunoprecipitated by anti-$p185^{HER2}$ antibody followed by immunoblotting with mouse anti-phosphotyrosine antibody (anti-PY) plus horseradish peroxidase-conjugated goat anti-mouse IgG (1:10,000 dilution) and ECL chemiluminescence reagent.

For detecting the recruitment of Grb2 and $p185^{HER2}$ into CD44v3 complex, SK-OV-3.ipl cells (either treated with HA (50 μg/ml) or without any HA treatment) were solubilized by Nonidet P-40 (as described above) and immunoprecipitated with anti-CD44v3 antibody followed by anti-Grb2 and/or $p185^{HER2}$-mediated immunoblot plus horseradish peroxidase-conjugated goat anti-mouse IgG (1:10,000 dilution) and ECL chemiluminescence reagent.

In some experiments, SK-OV-3.ipl cells (*e.g.* untransfected or transfected with HA1-tagged ΔN-Grb2 cDNA or HA1-tagged ΔC-Grb2 cDNA or vector only) were immunoblotted with various immunoreagents (*e.g.* rabbit anti-CD44v3 antibody, rabbit anti-Vav2 antibody, and mouse anti-$p185^{HER2}$ antibody) (5 μg/ml) for 1 h at room temperature followed by incubation with horseradish peroxidase-conjugated goat anti-rabbit IgG or mouse IgG (1:10,000 dilution) at room temperature for 1 h. Some SK-OV-3.ipl cells (*e.g.* untransfected or transfected by HA1-tagged ΔN-Grb2 cDNA or HA1-tagged ΔC-Grb2 cDNA or vector only) were also immunoprecipitated with anti-HA1 antibody followed by immunoblotting with anti-CD44v3 or anti-Vav2 or $p185^{HER2}$, respectively. These blots were then developed using ECL chemiluminescence reagent (Amersham Biosciences) according to the manufacturer's instructions. During these immunological analyses, an equal amount of cellular protein (50 μg/ml) immunoprecipitated with the antibody was applied to SDS-PAGE followed by immunoblot analyses.

Cloning, Expression, and Purification of CD44 Cytoplasmic Domain (CD44cyt) from Escherichia coli—The procedure for preparing the fusion protein of the cytoplasmic domain of CD44 was the same as described previously (12, 13, 16). Specifically, the cytoplasmic domain of human CD44 (CD44cyt) was cloned into pFLAG-AST using the PCR-based cloning strategy. By using human CD44 cDNA as template, one PCR primer pair (left, FLAG-*Eco*RI; right, FLAG-*Xba*I) was designed to amplify the complete CD44 cytoplasmic domain. The amplified DNA fragments were one-step-cloned into a pCR2.1 vector and sequenced. The DNA fragments were then cut out by double digestion with *Eco*RI and *Xba*I and subcloned into *Eco*RI/*Xba*I double-digested pFLAG-AST (Eastman Kodak Co.) to generate FLAG-pCD44cyt construct. The nucleotide sequence of FLAG/CD44cyt junction was confirmed by sequencing. The recombinant plasmids were transformed to BL21-DE3 to produce FLAG-CD44cyt fusion protein. The FLAG-CD44cyt fusion protein was further purified by anti-FLAG M2 affinity gel column (Kodak). The nucleotide sequences of primers used in this cloning protocol are as follows: FLAG-*Eco*RI, 5′-GAGAATTCGAACAGTCGAAGAAGGTGTCTCTTAAGC-3′; FLAG-*Xba*I, 5′-AGCTCTAGATTACACCCCAATCTTCAT-3′.

Expression Constructs—The cDNA fragment encoding the carboxyl-terminal SH3-SH2-SH3 domain of Vav2 (aa 594–878) was generated by RT-PCR using two specific primers, 5′-TGGAATTCTGGAACTGCTCCGGGGTGAC-3′ and 5′-AGCGGCCGCCTGGACGCCTTCCTCTTCCAC-3′. PCR product digested with *Eco*RI and *Hin*dIII was purified with QIAquick PCR purification Kit (Qiagen). The carboxyl-terminal SH3-SH2-SH3 Vav2 fragment cDNA was subsequently cloned into pcDNA3.1/HisC vector that contains Xpress-epitope to create His-tagged SH3-SH2-SH3 Vav2 fragment cDNA. The inserted SH3-SH2-SH3 domain sequence was confirmed by nucleotide sequencing analyses. This His-tagged SH3-SH2-SH3 Vav2 fragment cDNA was then used for transient expression in COS-7 cells or SK-OV-3ipl cells as described below. The His-tagged SH3-SH2-SH3 Vav2 fragment was expressed as a 30-kDa protein in COS-7 and SK-OV-3.ipl cells as detected by SDS-PAGE and immunoblot/immunoprecipitation analyses as described above.

ΔN-Grb2 is an amino-terminal SH3 domain deletion of Grb2. ΔC-Grb2 is a carboxyl-terminal SH3 domain deletion mutant of Grb2. The cDNAs encoding the ΔN-Grb2 and ΔC-Grb2 are driven by the cytomegalovirus promoter and preceded by the hemagglutinin epitope (HA1) tag in expression vector pCGN-Bam, which contains the hygromycin-resistant gene as a selection marker (55). These HA1-tagged ΔN-Grb2 cDNA or HA1-tagged ΔC-Grb2 cDNA were then used for transient expression in SK-OV-3ipl cells as described below. The truncated Grb2 products such as HA1-tagged ΔN-Grb2 or HA1-tagged ΔC-Grb2 were expressed as 22 or 20 kDa, respectively, as detected by SDS-PAGE and immunoblot analyses as described above.

Cell Transfection—To establish a transient expression system, various cell lines (*e.g.* COS-7 cells or SK-OV-3.ipl.cells) were transfected with various plasmid DNAs (*e.g.* His-tagged SH3-SH2-SH3 cDNA, HA1-tagged ΔN-Grb2, and ΔC-Grb2 cDNA or vector alone) using electroporation methods according to those procedures described previously (58). Briefly, cells were plated at a density of 2×10^6 cells per 100-mm dish and transfected with 25 μg/dish plasmid cDNA using electroporation at 230 V and 960 microfarads with a Gene Pulser (Bio-Rad). Transfected cells were grown in the culture medium for at least 24–48 h. Various transfectants were then analyzed for their protein expression (*e.g.* carboxyl-terminal Vav2 fragment and two truncated Grb2 proteins (ΔN-Grb2 or ΔC-Grb2)) by immunoblot and immunoprecipitation as described above.

In Vitro Binding of CD44cyt to the SH3-SH2-SH3 Vav2 Fragment or Intact Vav2—Aliquots (0.5–1 ng of protein) of purified His-tagged SH3-SH2-SH3 Vav2 fragment (isolated from COS-7 or SK-OV-3.ipl cells) or

intact Vav2 (purified from SK-OV-3.ipl cells)-conjugated Sepharose beads were incubated in 0.5 ml of binding buffer (20 mM Tris-HCl (pH 7.4), 150 mM NaCl, 0.1% bovine serum albumin and 0.05% Triton X-100) containing various concentrations (10–800 ng/ml) of ^{125}I-labeled cytoplasmic domains of CD44 (CD44cyt) fusion protein (5,000 cpm/ng protein) at 4 °C for 4 h. Specifically, equilibrium-binding conditions were determined by performing a time course (1–10 h) of ^{125}I-labeled CD44cyt binding to the SH3-SH2-SH3 Vav2 fragment or intact Vav2 at 4 °C. The binding equilibrium was found to be established when the *in vitro* CD44-(SH3-SH2-SH3 Vav2 fragment or intact Vav2) binding assay was conducted at 4 °C after 4 h. Following binding, the Vav2 fragment/intact Vav2-conjugated beads were washed extensively in binding buffer, and the beads-bound radioactivity was counted. Nonspecific binding was determined using a 50–100-fold excess of unlabeled CD44cyt in the presence of the same concentration of ^{125}I-labeled CD44cyt. Nonspecific binding, which was ~20% of the total binding, was always subtracted from the total binding. Our binding data are highly reproducible. The values expressed in Fig. 5 represent an average of triplicate determinations of 3–5 experiments with an S.D. less than ±5%.

In some cases, 0.1 μg of surface-biotinylated CD44 was incubated with various Vav2-related proteins (*e.g.* purified intact Vav2 or His-SH3-SH2-SH3-coated beads) in the presence and absence of 100-fold excess amount of His-SH3-SH2-SH3 at room temperature in the binding buffer (20 mM Tris-HCl (pH 7.4), 150 mM NaCl, 0.1% bovine serum albumin and 0.05% Triton X-100) for 1 h. After binding, biotinylated CD44 bound to the beads was analyzed by SDS-PAGE, transferred to the nitrocellulose filters, and incubated with ExtrAvidin-peroxidase (Sigma). After an addition of peroxidase substrate (Pierce), the blots were developed using ECL chemiluminescence reagent (Amersham Biosciences) according to the manufacturer's instructions.

Vav2-mediated GDP/GTP Exchange For Rac1 Proteins—Purified *E. coli*-derived GST-tagged Rac1 or GST alone (20 pmol) was preloaded with GDP (30 μM) in 10 μl of buffer containing 25 mM Tris-HCl (pH 8.0), 1 mM dithiothreitol, 4.7 mM EDTA, 0.16 mM $MgCl_2$, and 200 μg/ml bovine serum albumin at 37 °C for 7 min. In order to terminate preloading procedures, additional $MgCl_2$ was then added to the solution (reaching a final concentration of 9.16 mM) as described previously (16, 17, 59). Subsequently, 2 pmol of Vav2 (bound to anti-Vav2-conjugated Sepharose beads) isolated from SK-OV-3.ipl cells (untransfected or transfected with ΔN-Grb2 cDNA or ΔC-Grb2 cDNA or vector alone) grown in the presence or absence of HA (50 μg/ml) (or fibronectin (50 μg/ml) or control samples (nonspecific cellular material associated with preimmune serum-conjugated Sepharose beads)) was preincubated with 2.5 μM [^{35}S]GTPγS (≈1,250 Ci/mmol) (in the presence or absence of 2.25 μM GTPγS) for 10 min followed by adding 2.5 pmol of GDP-loaded GST-tagged Rac1 (or GDP-treated GST). At various time points, the reaction of each samples was terminated by adding ice-cold termination buffer containing 20 mM Tris-HCl (pH 8.0), 100 mM NaCl, and 10 mM $MgCl_2$ followed by filtering through nitrocellulose filters. The radioactivity associated with the filters was measured by scintillation fluid as described previously (16, 17, 59). The amount of [^{35}S]GTPγS bound to Vav2 (bound to anti-Vav2-Sepharose beads) or control sample (preimmune serum-conjugated Sepharose beads) in the absence of GST-tagged Rac1 was subtracted from the original values. In some cases, Vav2-catalyzed GDT/GTP exchange reactions were measured using SK-OV-3.ipl transfectants (or untransfected cells) preincubated with monoclonal rat anti-CD44 antibody (or normal rat IgG) followed by HA treatment or fibronectin treatment (or no treatment). Data represent an average of triplicates from 3 to 5 experiments. The standard deviation was less than 5%.

Analysis of Ras-bound Guanine Nucleotides—The procedures used in this assay were the same as those described previously (55, 60) with slight modifications. SK-OV-3.ipl cells (~1×10^4 cells) were first incubated with phosphate-free medium supplemented with 5% dialyzed serum followed by labeling with [^{32}P]orthophosphate (400 μCi/ml) in the same medium for 12 h. After washing with phosphate-buffered saline (PBS, pH 7.2), labeled cells were then incubated with HA (50 μg/ml) for various time intervals (*e.g.* 0, 2, 5, 10, 15, 20, 30, and 60 min). Subsequently, cells were solubilized in 50 mM HEPES (pH 7.5), 150 mM NaCl, 20 mM $MgCl_2$, 0.5% Nonidet P-40, 0.2 mM Na_3VO_4, 0.2 mM phenylmethylsulfonyl fluoride, 10 μg/ml leupeptin, and 5 μg/ml aprotinin followed by anti-Ras-mediated immunoprecipitation plus agarose bead-coated goat anti-rat IgG. The beads were extensively washed with lysis buffer, and proteins were solubilized in 1% SDS at 68 °C. The bound guanine nucleotides were chromatographed on polyethyleneimine-cellulose plates in 1.3 M LiCl. The GTP/GDP ratio was determined by a Betascope 603 Blot Analyzer (Betagen, Boston). The percentage of GTP-bound Ras in untransfected SK-OV-3.ipl cells (with no HA treatment control) was designated as 100%. Each assay was set up in triplicate and repeated at least 3 times. All data were analyzed statistically using the Student's *t* test and statistical significance was set at $p < 0.01$.

Binding of [^{3}H]Hyaluronan or ^{125}I-Fibronectin to SK-OV-3.ipl Cells—[^{3}H]HA was prepared from rat fibrosarcoma cells by D-[^{3}H]glucosamine labeling as described previously (5). Fibronectin (~2 μg of protein) was ^{125}I-labeled to a specific activity of 60,000 cpm/ng protein using the methods described by Frank and Speck (61). To test ligand binding, SK-OV-3.ipl cells (~4×10^5 cells) grown in 6-well culture plates were incubated with various concentrations (0.3–4.8 μg/ml) of [^{3}H]HA (1×10^5 dpm/μg) or ^{125}I-fibronectin (1×10^5 dpm/μg) in binding buffer (PBS containing 0.2% bovine serum albumin) at 4 °C for 4 h. In some cases, cells were first treated with monoclonal rat anti-CD44 antibody (50 μg/ml) at room temperature for 30 min followed by [^{3}H]HA or ^{125}I-fibronectin binding. Following binding, the cells were washed three times in the binding buffer and solubilized in 20 mM Tris-HCl (pH 7.4) solution containing 0.1% SDS. The radioactivity associated with solubilized cell extracts was counted in a liquid scintillation counter. The nonspecific binding was determined in presence of 100-fold excess of unlabeled HA (or unlabeled fibronectin) and was subtracted from the total binding.

In Vitro Tumor Cell Growth Assays—SK-OV-3.ipl cells (untransfected or transfected with various truncated Grb2cDNAs (*e.g.* ΔN-Grb2cDNA or ΔC-Grb2cDNA) or vector alone) (5×10^3 cells/well) were treated with HA (50 μg/ml) (or pre-treated with rat anti-CD44 followed by HA treatment (50 μg/ml) or untreated). These cells were then plated in 96-well culture plates in 0.2 ml of Dulbecco's modified Eagle's medium/F-12 medium supplement (Life Technologies, Inc.) containing either 0.5% fetal bovine serum or no serum for 24 h at 37 °C in 5% CO_2, 95% air. In each experiment, a total of 5 plates (10 wells/treatment (*e.g.* HA treatment or rat anti-CD44 plus HA treatment or no treatment)/plate) was used. Experiments were repeated three times. The *in vitro* growth of these cells were analyzed by measuring increases in cell number using the 3-(4,5-dimethylthiazol-2-yl)-2,5-diphenyltetrazolium bromide assays (CellTiter 96^R non-radioactive cell proliferation assay according to the procedures provided by Promega) (2). Subsequently, viable cell-mediated reaction products were recorded by a Molecular Devices (Spectra Max 250) enzyme-linked immunosorbent assay reader at a wavelength of 450 nm.

Tumor Cell Migration Assays—Twenty four transwell units were used for monitoring *in vitro* cell migration as described previously (16, 17). Specifically, the 5-μm porosity polycarbonate filters (CoStar Corp., Cambridge, MA) were used for the cell migration assay. SK-OV-3.ipl cells (~1×10^4 cells/well in PBS (pH 7.2) (in the presence or absence of rat anti-CD44 antibody (50 μg/ml)) were placed in the upper chamber of the transwell unit. In some cases, cells were transfected with various truncated Grb2cDNAs (*e.g.* ΔN-Grb2cDNA and ΔC-Grb2cDNA) or vector alone. The growth medium containing high glucose Dulbecco's modified Eagle's medium supplemented with 200 μg/ml hyaluronic acid was placed in the lower chamber of the transwell unit. After 18 h of incubation at 37 °C in a humidified 95% air, 5% CO_2 atmosphere, vital stain 3-(4,5-dimethylthiazol-2-yl)-2,5-diphenyltetrazolium bromide (Sigma) was added at a final concentration of 0.2 mg/ml to both the upper and the lower chambers and incubated for additional 4 h at 37 °C. Migrative cells at the lower part of the filter were removed by swabbing with small pieces of Whatman filter paper. Both the polycarbonate filter and the Whatman paper were placed in dimethyl sulfoxide to solubilize the crystal. Color intensity was measured in 450 nm. Cell migration processes were determined by measuring the cells that migrate to the lower side of the polycarbonate filters by standard cell number counting methods as described previously (16, 17). The CD44-specific cell migration was determined by subtracting nonspecific cell migration (*i.e.* cells migrate to the lower chamber in the presence of rat anti-CD44 antibody treatment) from the total migrative cells in the lower chamber. The CD44-specific cell migration in vector-transfected cells (control) is designated as 100%. Each assay was set up in triplicate and repeated at least 3 times. All data were analyzed statistically using the Student's *t* test, and statistical significance was set at $p < 0.01$.

RESULTS

Expression of CD44v3 and Vav2 In Human Ovarian Tumor Cells

CD44v3 Expression—The expression of CD44 variant (CD44v) isoforms is known to be closely correlated with onco-

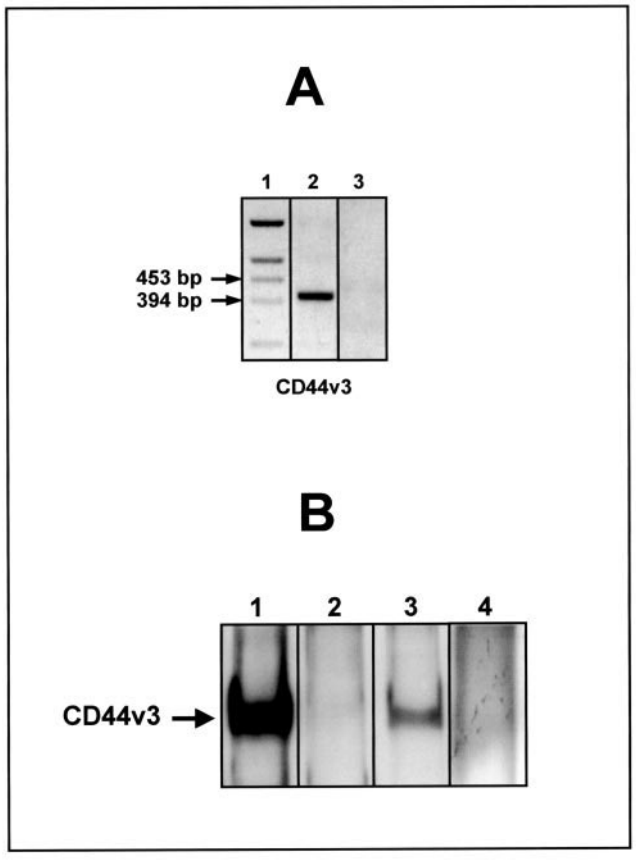

FIG. 1. **Characterization of CD44v3 expression in human ovarian tumor cells (SKOV3.ipl) by RT-PCR (*A*) and anti-CD44v3-immunoprecipitation analyses (*B*).** *A,* RT-PCR analysis. Total RNA isolated from human ovarian cells (SKOV3.ipl) was reverse-transcribed and subjected to PCR using CD44v3-specific primer pairs (*e.g.* exon 5 and v3 (exon 7) primer pairs) as described under "Materials and Methods." *Lane 1,* markers. *Lanes 2* and *3,* ethidium bromide staining of RT-PCR product detected in SK-OV-3.ipl cells in the presence (*lane 2*) and the absence of reverse transcriptase (*lane 3*). *B,* anti-CD44v3 antibody-mediated immunoprecipitation. Human ovarian cells (SK-OV-3.ipl) were surface-biotinylated, Nonidet P-40-solubilized, and immunoprecipitated by two different anti-CD44 antibodies as described under "Materials and Methods." *Lane 1,* immunoprecipitation of surface-biotinylated SKOV3.ipl cells using monoclonal rat anti-CD44 antibody (recognizing a common determinant of the CD44 class of glycoproteins, including variant isoforms). *Lane 2,* immunoprecipitation of surface-biotinylated SKOV3.ipl cells with normal rat IgG. *Lane 3,* immunoprecipitation of surface-biotinylated SKOV3.ipl cells using rabbit anti-CD44v3 antibody (recognizing a v3-specific sequence located at the membrane proximal region of the extracellular domain of CD44). *Lane 4,* immunoprecipitation of surface-biotinylated SKOV3.ipl cells with preimmune rabbit IgG.

genic signaling and metastatic behavior of a variety of tumor cells including human ovarian tumor cells (2, 11, 19). The question of what CD44v isoform(s) is expressed in human ovarian tumor cells (*e.g.* SK-OV-3.ipl cells) is addressed in this study. By using a PCR primer pair to amplify between exon 5 and v3 (exon 7) by RT-PCR, we have detected the presence of one major v3-containing PCR product of ≈400 bp (Fig. 1*A, lane 2*, based on markers indicated in Fig. 1*A, lane 1*) in SK-OV-3.ipl cells. This v3-containing PCR product was then "one-step-cloned" into the pCRII vector from Invitrogen Corp. (San Diego, CA) and sequenced. The nucleotide sequence confirms that this band belongs to the v3 exon insertion (data not shown). We believe that the RT-PCR is specific since no amplified fragment can be detected in samples incubated without reverse transcriptase (Fig. 1*A, lane 3*).

In order to characterize CD44 protein expression in the human ovarian tumor cells (SK-OV-3.ipl cell line), we have utilized surface biotinylation techniques followed by immunoprecipitation with a monoclonal rat anti-CD44 antibody (recognizing a common determinant of the CD44 class of glycoproteins, including various variant isoforms) (Fig. 1*B, lane 1*) or a rabbit anti-CD44v3 antibody (recognizing a v3-specific sequence located at the membrane proximal region of the extracellular domain of CD44) (Fig. 1*B, lane 3*). Our results indicate that a single surface-biotinylated polypeptide (≈85 kDa) displaying immunological cross-reactivity with CD44 is preferentially expressed on the cell surface of human ovarian tumor cells (Fig. 1*B, lanes 1* and *3*). In particular, an anti-CD44v3 antibody capable of immunoprecipitating the 85-kDa surface-biotinylated protein (Fig. 1*B, lane 3*) further confirms that the CD44v3 protein is expressed on the surface of SK-OV-3.ipl cells. No CD44-containing material is observed in control samples when normal rat IgG or preimmune rabbit IgG is used in these experiments (Fig. 1*B, lane 2* or *lane 4*).

TABLE I

Effect of monoclonal rat anti-CD44 antibody on ligand binding (e.g. [^{3}H]-HA binding or [^{125}I]-fibronectin binding) in ovarian tumor cells (SK-OV-3.ipl cells)

Treatments	[^{3}H]HA Binding	^{125}I-Fibronectin binding
	% control[a]	
No treatment (control)	100	100
Normal rat IgG	97	101
Rat anti-CD44 IgG	29	99

[a] SK-OV-3.ipl cells were either untreated (control) or pretreated with rat anti-CD44 IgG (50 μg/ml) or normal rat IgG (50 μg/ml) at room temperature for 30 min followed by incubating with either [^{3}H]HA (1 μg/ml) or ^{125}I-fibronectin (1 μg/ml) at 4 °C for 2 h in PBS. The nonspecific binding was determined in the presence of unlabeled HA (100 μg/ml), or unlabeled fibronectin (100 μg/ml) was subtracted. The specific binding observed in no treatment (control) is designated as 100%.

To determine whether CD44v3 is involved in HA binding, SK-OV-3.ipl cells were preincubated with a monoclonal rat anti-CD44 antibody that recognizes a common determinant of the CD44 class of glycoproteins including CD44v3 isoform followed by the addition of [^{3}H]HA. As shown in Table I, monoclonal rat anti-CD44 antibody (50 μg/ml) (but not normal rat IgG control (50 μg/ml)) significantly inhibits [^{3}H]HA binding. In controls, SK-OV-3.ipl cells were also incubated with ^{125}I-fibronectin. Our data also show that neither rat anti-CD44 antibody nor normal rat IgG is capable of blocking the interaction between certain surface molecule(s) and fibronectin (Table I). These findings support the notion that CD44v3 is the major HA receptor (but not the fibronectin receptor) on ovarian tumor cells. The v3 (or exon 7) insertion in the CD44v3 isoform has also been shown to contain heparin sulfate addition sites (62) required for the binding of heparin-binding growth factors, cytokines, and chemokines that promote tumor progression (11, 63). These observations prompted our laboratory to examine CD44v3-associated oncogenic signaling in human ovarian tumor cells.

Vav2 Expression—Several lines of evidence support the notion that the Vav family of GEFs (dbl molecules) is involved in RhoGTPase activation, cytoskeleton function, and cellular transformation (30, 37–40). To examine the expression of Vav2 transcripts in human ovarian tumor cells, total RNA from SK-OV-3.ipl cells was isolated and analyzed by RT-PCR using Vav2-specific primer pairs. Employing ethidium bromide staining of agarose gels, we have identified a major PCR product of 1500 bp corresponding to Vav2 (Fig. 2*A*, *lane 2*, based on markers indicated in Fig. 2*A, lane 1*) in SK-OV-3.ipl cells. No amplified fragment is detected in samples incubated without reverse transcriptase (Fig. 2*A, lane 3*), indicating that the

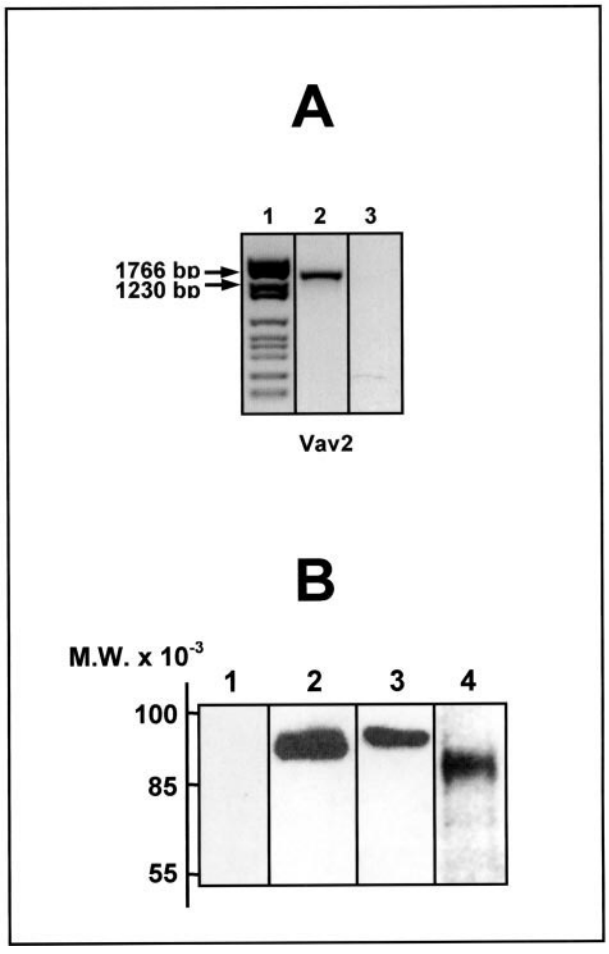

FIG. 2. **Detection of Vav2 and Vav2-CD44v3 complex in SK-OV-3.ipl cells.** *A,* RT-PCR analysis. Total RNA isolated from human ovarian cells (SKOV3.ipl) was reverse-transcribed and subjected to PCR using Vav2-specific primer pairs as described under "Materials and Methods." *Lane 1,* markers. *Lanes 2* and *3,* ethidium bromide staining of RT-PCR product detected in SK-OV-3.ipl cells in the presence (*lane 2*) and the absence of reverse transcriptase (*lane 3*). *B,* Vav2-CD44v3 complex analysis. SK-OV-3.ipl cells were solubilized by 1% Nonidet P-40 buffer followed by immunoprecipitation and/or immunoblot by anti-Vav2 antibody or anti-CD44v3 antibody, respectively, as described under "Materials and Methods." *Lane 1,* immunoblot of SK-OV-3.ipl cells with preimmune rabbit IgG. *Lane 2,* detection of Vav2 with anti-Vav2-mediated immunoblot of SK-OV-3.ipl cells. *Lane 3,* detection of Vav2 in the complex by anti-CD44v3 immunoprecipitation followed by immunoblotting with anti-Vav2 antibody. *Lane 4,* detection of CD44v3 in the complex by anti-Vav2 immunoprecipitation followed by immunoblotting with anti-CD44v3 antibody.

RT-PCR is specific. Our data clearly demonstrate that the Vav2 transcript is expressed in human ovarian tumor cells.

Since gene expression at the mRNA level does not always correlate with cellular protein expression, it is important to determine whether Vav2 protein expression occurs in the human ovarian tumor cells. Immunoblot analysis, utilizing an anti-Vav2 antibody designed to recognize a Vav2-specific sequence, reveals a single polypeptide (≈95 kDa) (Fig. 2*B, lane 2*). We have also demonstrated that the Vav2 protein detected by anti-Vav2-mediated immunoblot is specific since no protein is detected in these cells incubated with preimmune rabbit IgG (Fig. 2*B, lane 1*). These results clearly indicate that Vav2 is expressed at both the transcript and protein levels in SK-OV-3.ipl cells.

Association between CD44v3 and Vav2 In Human Ovarian Tumor Cells

Next we addressed the question of whether there is a direct interaction between CD44v3 and Vav2 in human ovarian tumor cells. First, we carried out both anti-CD44v3-mediated and anti-Vav2-mediated precipitation followed by anti-Vav2 immunoblot (Fig. 2*B, lane 3*) or anti-anti-CD44v3 immunoblot (Fig. 2*B, lane 4*), respectively. Our results demonstrate that the Vav2 band is revealed in anti-CD44v3-immunoprecipitated materials (Fig. 2*B, lane 3*), and the CD44v3 band is detected in the anti-Vav2-immunoprecipitated materials (Fig. 2*B, lane 4*). These findings suggest that CD44v3 and Vav2 are physically associated in ovarian tumor cells.

Previous studies have indicated that the SH3-SH2-SH3 domain of Vav2 is involved in protein-protein interactions (64–67) during growth factor receptor-mediated cellular signaling (68). To determine whether there is a direct interaction between CD44 and Vav2, we have prepared a purified recombinant SH3-SH2-SH3 fragment of Vav2 and a FLAG-tagged cytoplasmic domain of CD44 (FLAG-CD44cyt) fusion protein for *in vitro* binding analysis with these two molecules. Specifically, we incubated ^{125}I-labeled FLAG-CD44cyt with the SH3-SH2-SH3 fragment of Vav2 (or an intact Vav2) under equilibrium binding conditions. Scatchard plot analyses presented in Fig. 3 indicate that the SH3-SH2-SH3 fragment of Vav2 binds to the cytoplasmic domain of CD44 (CD44cyt) at a single site with high affinity (an apparent dissociation constant (K_d) of ≈1.87 nM) (Fig. 3*A*). This interaction between CD44 and the SH3-SH2-SH3 fragment of Vav2 is comparable in affinity to CD44 binding to intact Vav2 (K_d ≈1.98 nM) (Fig. 3*B*). These findings clearly establish the fact the SH3-SH2-SH3 domain of Vav2 contains the CD44-binding site.

Vav2-catalyzed Rac1 Activation in SK-OV-3.ipl Cells

It has been reported that Vav2 functions as an exchange factor for Rho-like GTPases such as Rac1 (34, 40–42). To confirm that the Vav2-like molecule in this study functions as a GDP/GTP exchange factor (or a GDP-dissociation stimulator (GDS) protein) for RhoGTPases, we first isolated Vav2 from SK-OV-3.ipl cells using anti-Vav2-conjugated Sepharose beads. As indicated in Fig. 4, the isolated Vav2 activates GDP/GTP exchange on GST-tagged Rac1 (Fig. 4). The initial onset of the exchange reaction on GST-tagged Rac1 occurs within 1–2 min after the addition of Vav2, and the reaction reaches its maximum ~10 min after Vav2 addition (Fig. 4*b*). Most importantly, we have observed that the addition of HA to CD44v3-containing SK-OV-3.ipl cells stimulates both the rate of Vav2-mediated GDP/GTP exchange reaction and the maximal amount of bound [^{35}S]GTPγS to GST-Rac1 (at least a 1.5-fold increase) (Fig. 4, *curve a*) as compared with Vav2 isolated from untreated SK-OV-3.ipl cells (Fig. 4, *curve b*). In control samples, a low level of [^{35}S]GTPγS-bound material was detected in GST alone under the same GDP/GTP exchange reaction using Vav2 isolated from SK-OV-3.ipl cells in the presence (Fig. 4*c*) or absence (Fig. 4*d*) of HA treatment. Therefore, we conclude that Vav2 in SK-OV-3.ipl cells functions as a GDP/GTP exchange factor for Rho-like GTPases such as Rac1GTPase.

It is also noted that the amount of [^{35}S]GTPγS-bound material detected in these samples isolated from SK-OV-3.ipl cells pretreated with rat anti-CD44 (but not normal rat IgG) followed by HA treatment was significantly reduced (Table II). Since other extracellular matrix components such as fibronectin fail to promote CD44-specific Vav2-mediated Rac1 activation (Table II), we believe that the binding of HA to CD44v3-containing SK-OV-3.ipl cells is directly involved in Vav2-mediated Rac1 activation.

CD44v3-Vav2 Interaction with the Grb2-p185^{HER2} Complex

The adaptor molecule, Grb2, contains a single SH2 domain and two SH3 domains (Fig. 6*A*) and is a key component in Ras

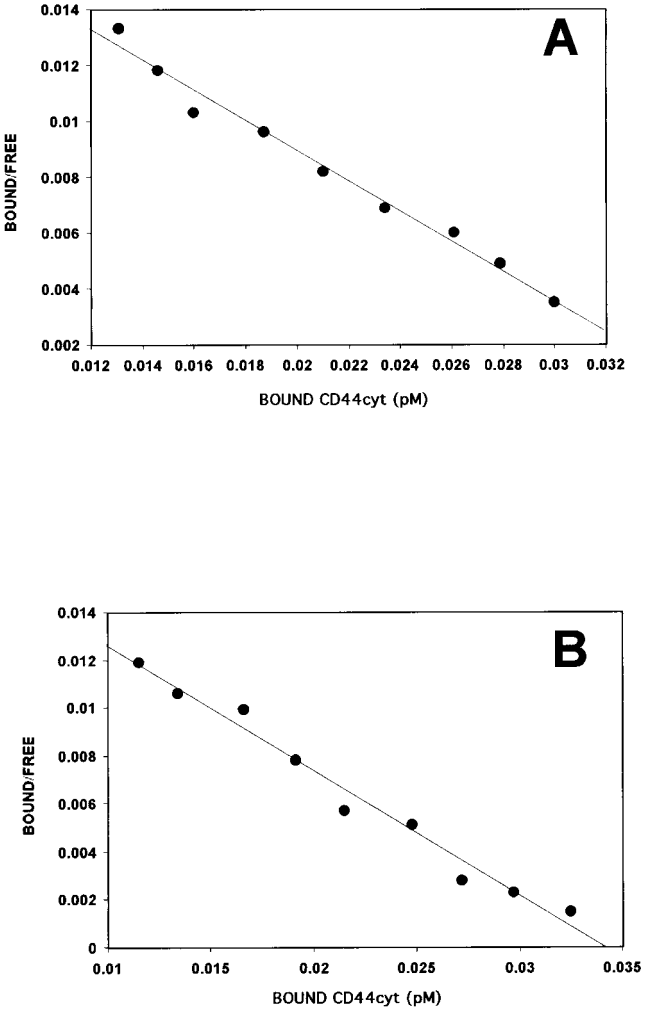

FIG. 3. **Binding of ^{125}I-labeled FLAG-CD44cyt to the SH3-SH2-SH3 fragment of Vav2 (or intact Vav2).** Various concentrations of ^{125}I-labeled FLAG-CD44cyt were incubated with the SH3-SH2-SH3 fragment of Vav2 (*A*) or intact Vav2 (*B*)-coupled beads at 4 °C for 4 h. Following binding, beads were washed extensively in binding buffer, and the bead-bound radioactivity was counted. As a control, ^{125}I-labeled FLAG-CD44cyt was also incubated with uncoated beads to determine the binding observed due to the nonspecific binding of the ligand. Nonspecific binding, which represented ~20% of the total binding, was always subtracted from the total binding. Our binding data are highly reproducible. The values expressed under "Results" represent an average of triplicate determinations of 3–5 experiments with an S.D. less than ±5%. *A,* Scatchard plot analysis of the equilibrium binding data between ^{125}I-labeled FLAG-CD44cyt and the SH3-SH2-SH3 fragment of Vav2. *B,* Scatchard plot analysis of the equilibrium binding data between ^{125}I-labeled FLAG-CD44cyt and intact Vav2.

signaling activated by receptor tyrosine kinases including p185^{HER2} (48–54). Several studies also show that Grb2 is capable of binding to Vav directly (69, 70). To examine the possible relationship between the CD44v3-Vav2 complex and other important signaling molecules such as p185^{HER2} and Grb2, we have analyzed the anti-CD44v3-mediated immunoprecipitates from cell lysate by immunoblotting with anti-p185^{HER2} (Fig. 5*B, a*) or anti-Grb2 (Fig. 5*B, b*) antibody, respectively. Our results demonstrate that both p185^{HER2} (Fig. 5*B, a, left lane*) and Grb2 (Fig. 5*B, b, left lane*) are complexed with the CD44v3 (together with Vav2) (Fig. 5*B, c* and *d, left lanes*). Furthermore, we have observed that HA treatment of SK-OV-3.ipl cells stimulates p185^{HER2} tyrosine kinase activity (Fig. 5*A*) and causes a significant increase in the amount of p185^{HER2} (Fig. 5*B, a, right lane*), Grb2 (Fig. 5*B, b, right lane*), and Vav2 (Fig. 5*B, c, right lane*), recruited into the CD44v3-associated (Fig. *B, d, right lane*) signaling complex leading to Ras activation (Table III), tumor cell growth (Table IV), and migration (Table V). These observations strongly suggest that HA interaction with CD44v3-Vav2 complex is capable of assembling other signaling molecules (*e.g.* p185^{HER2} and Grb2) into a large complex for the activation of multiple signaling pathways including both Rac1 and Ras pathways during ovarian tumor cell functions.

A previous study found that deletion of the amino-SH3 domain (designated as ΔN-Grb2), but not the carboxyl-SH3 domain of Grb2 (designated as ΔC-Grb2), interrupts the protein-protein interactions between Grb2 and p185^{HER2} resulting in an inhibition of oncogenic signaling by activated p185^{HER2} and a reversal of the transformed phenotype (55). In order to examine the role of Grb2 in regulating CD44v3-Vav2 and p185^{HER2}-mediated oncogenic signaling in human ovarian tumor cells (SK-OV-3.ipl cells), we have transfected SK-OV-3.ipl cells with HA1-tagged ΔN-Grb2cDNA, HA1-tagged ΔC-Grb2cDNA (Fig. 6*A*), or vector alone. Our results with these three transfectants indicate that both ΔN-Grb2 and ΔC-Grb2 are expressed in SK-OV-3.ipl cells as determined by anti-HA1-mediated immunoprecipitation followed by anti-HA1 immunoblot (Fig. 6*C, d, lanes 1* and *2*). No protein band was revealed in vector-transfected SK-OV-3.ipl cells using the same anti-HA1 immunoprecipitation and immunoblot procedures (Fig. 6*C, d, lane 3*). Apparently, CD44v3 (Fig. 6*B, a, lanes 1–3*), Vav2 (Fig. 6*B, b, lanes 1–3*), and p185^{HER2} (Fig. 6*B, c, lanes 1–3*) are expressed at comparable levels in all three transfectants. By using anti-HA1-mediated immunoprecipitation of SK-OV-3.ipl cells transfected with HA1-tagged ΔC-Grb2cDNA followed by immunoblotting with various antibodies (*e.g.* anti-CD44v3, anti-Vav2, or anti-p185^{HER2} antibody), we have found that all three molecules (*i.e.* CD44v3 (Fig. 6*C, a, lane 1*), Vav2 (Fig. 6*C, b, lane 1*), and p185^{HER2} (Fig. 6*C, c, lane 1*)) are co-precipitated with HA1-tagged ΔC-Grb2 (Fig. 6*C, d, lane 1*) in these transfectants. We believe that the CD44v3, Vav2, and p185^{HER2} detected in the anti-HA1-mediated immunoprecipitated materials are specific since no protein (Fig. 6*C, a–c, lane 3*) is detected in vector-transfected cells using the same immunoprecipitation procedures (Fig. 6*C, d, lane 3*). We have also shown that very little CD44v3 (Fig. 6*C, a, lane 2*), Vav2 (Fig. 6, *b, lane 2*), and p185^{HER2} (Fig. 6, *c, lane 2*) is present in anti-HA1-mediated immunoprecipitated materials (Fig. 6*C, d, lane 2*) isolated from SK-OV-3.ipl cells transfected with HA1-tagged ΔN-Grb2cDNA (Fig. 6*C, lane 2*). These observations indicate that the amino-SH3 (but not the carboxyl-SH3) of Grb2 is important for the binding of p185^{HER} and is also required for its interaction with the CD44v3-Vav2 complex.

Furthermore, we have demonstrated that transfection of SK-OV-3.ipl cells with ΔC-Grb2 cDNA does not cause any change in HA-dependent, Vav2-catalyzed GDP/GTP exchange reaction on Rac1 (Fig. 7, *curves b* and *d*) and Ras activation (Table III) as well as the ovarian tumor cell-specific properties (*e.g.* cell growth (Table IV) and migration (Table V)), as compared with vector-transfected cells (Fig. 7, *curves a* and *c*; Tables III–V). However, overexpression of ΔN-Grb2 (by transfection of SK-OV-3.ipl cells with ΔN-Grb2cDNA) significantly impairs HA-mediated Vav2-Rac1 signaling (Fig. 7, *curves e* and *f*) and Ras activation (Table III) as well as ovarian tumor cell growth (Table IV) and migration (Table V). These data support the conclusion that CD44-Vav2 interaction with the Grb2-p185^{HER2} complex plays an important role in promoting HA-dependent Rac1 activation and Ras signaling leading to the concomitant stimulation of human ovarian tumor cell migration and growth.

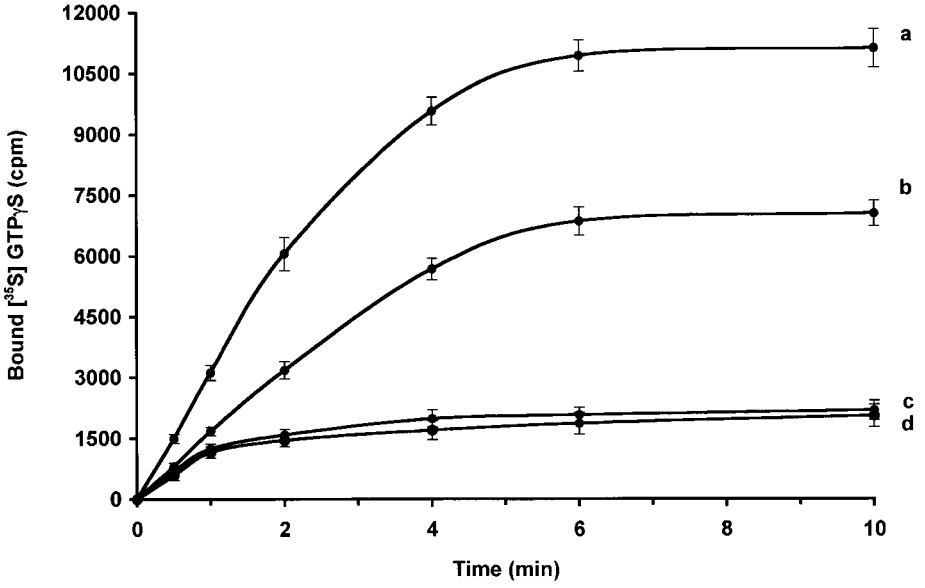

FIG. 4. **Vav2-mediated GDP/GTP exchange for Rac1 protein.** Vav2 isolated from SK-OV-3.ipl cells (treated with HA or without any treatment) was preincubated for 10 min with 0.25 μM [^{35}S]GTPγS (1,250 Ci/mmol) and 2.25 μM GTPγS (or in the presence of 1 mM unlabeled GTPγS) followed by adding GDP-loaded GST-Rac1 GTPases (or GST alone). The amount of [^{35}S]GTPγS bound to samples in the absence of GTPases was subtracted from the original values. Data represent an average of triplicates from 3 to 5 experiments. The S.D. was less than 5%. *Curve a,* kinetics of [^{35}S]GTPγS bound to GDP-loaded GST-tagged Rac1 in the presence of Vav2 (isolated from SK-OV-3.ipl cells treated with HA). *Curve b,* kinetics of [^{35}S]GTPγS bound to GDP-loaded GST-tagged Rac1 in the presence of Vav2 (isolated from SK-OV-3.ipl cells without any HA treatment). *Curve c,* kinetics of [^{35}S]GTPγS bound to GDP-treated GST in the presence of Vav2 (isolated from SK-OV-3.ipl cells treated with HA). *Curve d,* kinetics of [^{35}S]GTPγS bound to GDP-treated GST in the presence of Vav2 (isolated from SK-OV-3.ipl cells without any HA treatment).

TABLE II
Effect of monoclonal rat anti-CD44 antibody on CD44v3-associated Vav2-mediated Rac1 activation in ovarian tumor cells (SK-OV-3.ipl cells)

Treatments	Amount of [^{35}S]GTPγS bound to GST-Rac1	
	No HA treatment	HA treatment
	pmol[a]	
No treatment (control)	1.35	2.01
Normal rat IgG	1.34	1.95
Rat anti-CD44 IgG	1.32	1.38

Treatments	Amount of [^{35}S]GTPγS bound to GST-Rac1	
	No fibronectin treatment	Fibronectin treatment
	pmol[a]	
No treatment (control)	1.36	1.41
Normal rat IgG	1.33	1.35
Rat anti-CD44 IgG	1.34	1.39

[a] Procedures for measuring CD44v3-associated Vav2-catalyzed GDP/GTP exchange reaction on GST-Rac1 were described under "Materials and Methods." Each assay was set up in triplicate and repeated at least three times. All data were analyzed statistically by Student's *t* test, and statistical significance was set $p < 0.01$. The values expressed in this table represent an average of triplicate determinations of three to five experiments with an S.D. of less than 5%.

DISCUSSION

CD44, which exists in a number of different isoforms, has been detected on the surface of ovarian cancer cells causing very strong adhesion to peritoneal mesothelium (24). Overexpression of certain CD44 isoforms on the tumor cell surface is closely associated with the progression of various carcinomas including ovarian cancers (2, 19, 71, 72). By using both RT-PCR (Fig. 1*A*) and immunoblot analyses (Fig. 1*B*), we have found that one of the major CD44 isoforms expressed on the surface of human ovarian tumor cells (*e.g.* SK-OV-3.ipl cell line) is the CD44v3 isoform. It has been speculated that the CD44v3 isoform on epithelial tumor cells may act as surface modulators to facilitate unwanted growth factor receptor-growth factor interactions (11, 62, 63) and subsequent tumor formation. It is also possible that the CD44v3 isoform interacts with extracellular matrix materials (*e.g.* hyaluronan (HA)) such that the epithelial tumor cells undergo abnormal growth and migration. Consequently, CD44v3 appears to play an important role in oncogenic signaling leading to tumor cell-specific phenotypes in a variety of human solid neoplasms, particularly those of gynecologic origin such as ovarian cancers (71, 72).

Several mechanisms have been suggested for the regulation of CD44-mediated functions. These include (i) modification by the addition of an extra exon-coded structure (via an alternative splicing process) (1, 11), (ii) variable *N-/O*-linked glycosylation on the extracellular domain of the CD44 (3–5), and (iii) modulation of the cytoplasmic domain of CD44 by fatty acylation (73), GTP binding (74), protein kinase C (4, 75), and/or Rho kinase-mediated phosphorylation (15). Previously, it has been shown that the binding of HA to CD44 stimulates Ca^{2+} mobilization (77) and CD44-cytoskeleton interaction (10, 77) followed by increased cell adhesion (77), proliferation (5), and migration (13, 15, 17, 19). All of these findings suggest that the extracellular domain of CD44 is required for cellular signaling events and that the cytoplasmic domain of CD44 interacts closely with cytoskeletal proteins (9–13, 56) and various signaling molecules (15, 17, 19) during the regulation of CD44-specific, HA-dependent functions. In particular, the cytoplasmic domain of CD44 isoforms selects its unique downstream effectors (*e.g.* cytoskeletal proteins, ankyrin (9–13, 56), or various oncogenic signaling molecules, Tiam1 (17), RhoA-activated Rho kinase (15), and c-Src kinase (19)) and coordinates intracellular signaling pathways leading to multiple cellular functions during tumor progression.

CD44v3-mediated oncogenesis is frequently regulated by activation of RhoGTPases such as Rac1 and RhoA (15, 17). In particular, Rac1 activation initiates oncogenic signaling pathways that are closely associated with cell shape changes (78, 79), actin cytoskeleton reorganization (78, 79), gene expression (80, 81), and tumor cell invasion/migration (16, 17). It has been well established that HA binding to CD44 promotes Rac1 acti-

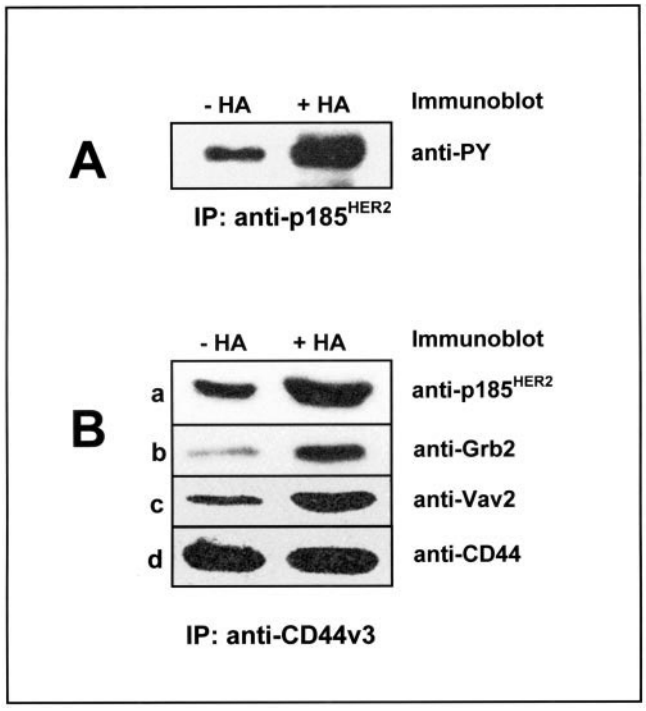

FIG. 5. **Detection of p185^{HER2} tyrosine phosphorylation and Grb2-p185^{HER2} recruitment to CD44v3 in HA-treated SK-OV-3.ipl cells.** *A,* detection of p185^{HER2} tyrosine phosphorylation. SK-OV-3.ipl cells (either treated with 50 μg/ml HA for 10 min (*right lane*) or without any HA treatment (*left lane*)) were solubilized and immunoprecipitated (*IP*) by anti-p185^{HER2} antibody followed by immunoblotting with mouse anti-phosphotyrosine antibody (*anti-PY*) as described under "Materials and Methods." *B,* recruitment of p185^{HER2}, Grb2, and Vav2 into CD44v3 complex detected by anti-CD44v3-mediated immunoprecipitation followed by anti-p185^{HER2} (*a*), anti-Grb2 (*b*), anti-Vav2 (*c*), and anti-CD44-mediated (*d*) immunoblot using SK-OV-3.ipl cells treated with 50 μg/ml HA (*right lane*) or without any HA (*left lane*).

TABLE III
Measurement of HA-mediated Ras activation in ovarian tumor cells SK-OV-3.ipl cells

Cells	GTP-bound Ras/(GDP-bound Ras + GTP-bound Ras) (%)[a]	
	No HA treatment	HA treatment
	% control	
Untransfected cells (control)	100	158
Vector-transfected cells	98	155
ΔC-Grb2cDNA-transfected cells	90	154
ΔN-Grb2cDNA-transfected cells	40	46

[a] Procedures for measuring Ras activation in SK-OV-3.ipl cells transfected with either ΔC-Grb2cDNA or ΔN-Grb2cDNA or vector alone were described under "Materials and Methods." Each assay was set up in triplicate and repeated at least 3 times. All data were analyzed statistically by Student's *t* test and statistical significance was set at $p < 0.01$. The values expressed in this table represent an average of triplicate determinations of 3–5 experiments with an S.D. of less than ± 5%.

vation (17, 18). In particular, the interaction between the CD44v3 isoform and one of the guanine nucleotide exchange factors, Tiam1, up-regulates Rac1 signaling and cytoskeleton-mediated metastatic breast tumor progression (17). In this study our aim was to identify CD44v3-linked molecules in human ovarian tumor cells whose expression correlates with HA-mediated metastatic behavior.

Vav is one of the GEFs that are identified as an oncogene by its ability to up-regulate RhoGTPase activity during malignant transformation (27, 37–40). Vav was first isolated in the course of gene transfer assays using human tumor DNA (28) and has been shown to activate multiple RhoGTPases (*e.g.* Rac1, Cdc42, RhoA, RhoB, and RhoG) (27, 37–40). The expression of Vav

TABLE IV
Measurement of HA-mediated growth of ovarian tumor cells (SK-OV-3.ipl cells)

Cells	Tumor cell growth	
	No HA treatment	HA treatment
	% control[a]	
Untransfected cells (control)	100	159
Vector-transfected cells	96	155
ΔC-Grb2cDNA-transfected cells	94	149
ΔN-Grb2cDNA-transfected cells	45	48

[a] Procedures for measuring ovarian tumor cell growth in SK-OV-3.ipl cells transfected with either ΔC-Grb2cDNA or ΔN-Grb2cDNA or vector alone were described under "Materials and Methods." Each assay was set up in triplicate and repeated at least 3 times. All data were analyzed statistically by Student's *t* test, and statistical significance was set at $p < 0.01$. The values expressed in this table represent an average of triplicate determinations of 3–5 experiments with an S.D. less than ± 5%.

TABLE V
Measurement of HA-mediated migration of ovarian tumor cells (SK-OV-3.ipl cells)

Cells	Tumor cell migration	
	No HA addition	HA addition
	% control[a]	
Untransfected cells (control)	100	155
Vector-transfected cells	98	150
ΔC-Grb2cDNA-transfected cells	95	150
ΔN-Grb2cDNA-transfected cells	44	51

[a] SK-OV-3.ipl cells ($\approx 1 \times 10^4$ cells/well in phosphate-buffered saline (PBS), pH 7.2) were placed in the upper chamber of the transwell unit. In some cases, SK-OV-3.ipl cells were transfected with either ΔC-Grb2cDNA-transfected cDNA, ΔN-Grb2cDNA-transfected cDNA, or vector alone. After 18 h of incubation at 37 °C in a humidified 95% air, 5% CO_2 atmosphere, cells on the upper side of the filter were removed by wiping with a cotton swap. Cell migration processes were determined by measuring the cells that migrate to the lower side of the polycarbonate filters containing HA (or no HA) by standard cell number counting assays as described under "Materials and Methods." The CD44-specific cell migration was determined by subtracting non-specific cell migration (*i.e.* cells migrate to the lower chamber in the presence of anti-CD44v3 antibody treatment) from the total migrative cells in the lower chamber. The CD44-specific cell migration in vector-transfected cells (control) is designated as 100%. Each assay was set up in triplicate and repeated at least three times. All data were analyzed statistically using the Student's *t* test, and statistical significance was set at $p < 0.01$. The values expressed in this table represent an average of triplicate determinations of 3–5 experiments with an S.D. less than ± 5%.

(also called Vav1) is restricted to hematopoietic system, whereas Vav2 (a homologue of Vav1) is widely expressed in a number of different cell types (29, 30). Our laboratory has demonstrated that Vav2 is expressed at both the RNA (Fig. 2*A*) and protein (Fig. 2*B*) levels in human ovarian tumor cells such as SK-OV-3.ipl cells. Specifically, Vav2 is identified as a 95-kDa protein (Fig. 2*B*) that is capable of carrying out GDP/GTP exchange on Rac1 (Fig. 4) in a manner similar to Vav2 described in other cell types (34, 40–42, 65, 66). In contrast, the initial rate of Vav2-catalyzed GDP/GTP exchange on GST-tagged Cdc42 and GST-tagged RhoA is significantly slower than that detected on Rac1 (data not shown). Therefore, we believe that Vav2 isolated from SK-OV-3.opl cells functions as an exchange factor for the Rho-like GTPases such as Rac1 (and to a lesser extent for RhoA and Cdc42).

The Vav2 molecule contains several functional domains including an amino-terminal leucine-rich and acid-rich domain (31), a DH domain (32, 33), a PH domain (34), a cysteine-rich zinc-binding domain (31), and two SH3 domains flanking a single SH2 domain (the carboxyl-terminal SH3-SH2-SH3 domain) (35, 36). In particular, the DH domain of Vav2 by itself exhibits GDP/GTP exchange activity for specific members of the Ras superfamily of GTP-binding proteins (32, 33) and plays

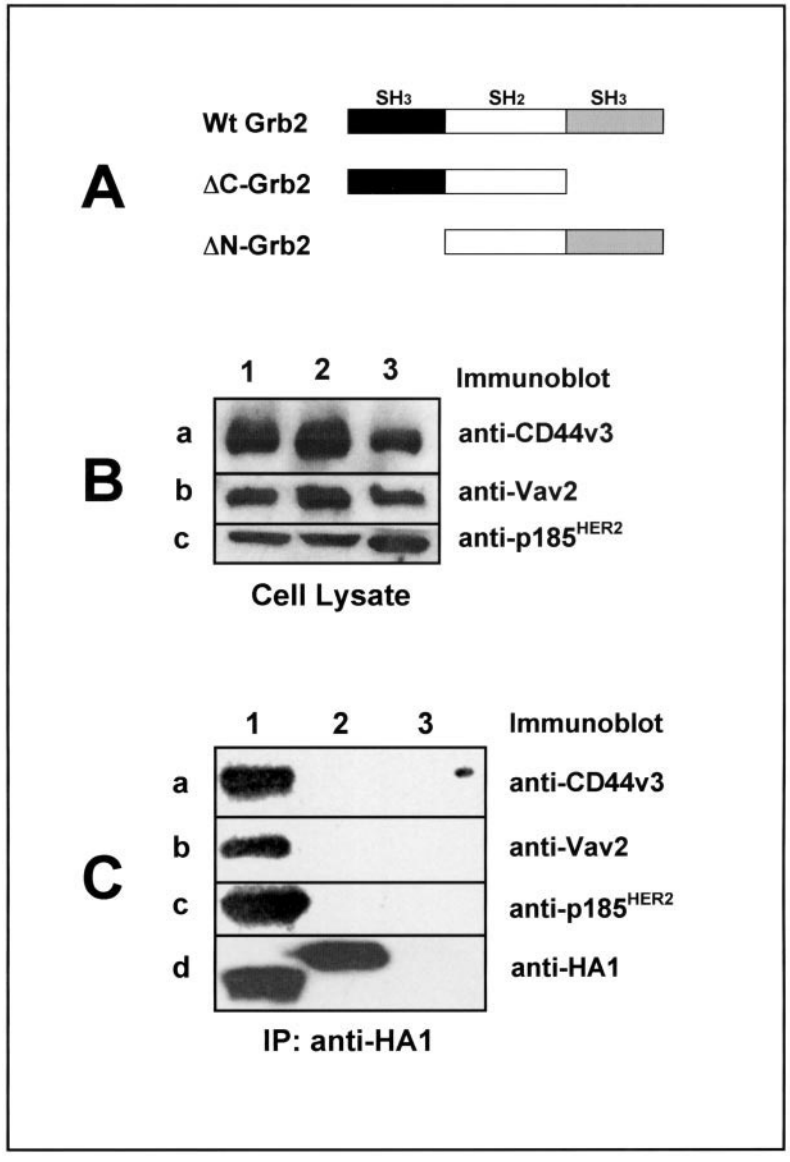

FIG. 6. **Transfection of SK-OV-3.ipl cells with ΔC-Grb2cDNA or ΔN-Grb2cDNA.** *A,* schematic illustration of both wild-type Grb2 (one SH2 domain flanked by two SH3 domains) and Grb2 deletion mutants (*e.g.* the ΔC-Grb2 mutant contains only the SH2 and the amino-terminal SH3 domain, whereas the ΔN-Grb2 mutant contains only the SH2 and the amino-terminal SH3 domain). *B,* detecting the expression of CD44v3, Vav2, and $p185^{HER2}$ by anti-CD44v3 (*a*), Vav2 (*b*), or anti-$p185^{HER2}$-mediated immunoblot (*c*), respectively, in the cell lysate obtained from HA1-tagged ΔC-Grb2cDNA (*lane 1, a–c*), ΔN-Grb2cDNA (*lane 2, a–c*), or in vector-transfected cells (*lane 3, a–c*). *C,* analysis of the signaling complex formation. SK-OV-3.ipl cells transfected with HA1-tagged ΔC-Grb2cDNA (*lane 1*), ΔN-Grb2cDNA (*lane 2*), or vector alone (*lane 3*) were solubilized by Nonidet P-40 (as described above) and immunoprecipitated with anti-HA1 antibody followed by immunoblotting with various immunoreagents (*e.g.* anti-CD44v3 (*a*), anti-Vav2 (*b*), anti-$p185^{HER2}$ (*c*), or anti-HA1 (*d*), respectively).

an important role in RhoGTPase signaling and cellular transformation (30). A number of laboratories have reported that the carboxyl-terminal SH3-SH2-SH3 domain interacts with a diverse array of proteins (*e.g.* Grb2 (69, 70), heterogeneous ribonuclear proteins K and C (65), nuclear protein Ku-70 (66), and the cytoskeletal protein Zyxin (67)). This sequence is also required for Vav2 targeting to the plasma membrane and activation of c-Jun NH_2-terminal kinase I (82). At the present time, identification of the membrane protein(s) involved in Vav2 binding remains to be accomplished.

In this study we have presented new evidence for a close, physical interaction between Vav2 and the transmembrane glycoprotein, CD44v3 isoform. First, we have shown that both Vav2 and CD44v3 are physically associated as a complex *in vivo* (Fig. 2*B*). By using two recombinant proteins, the carboxyl-terminal SH3-SH2-SH3 domain of Vav2 and the cytoplasmic domain of CD44, we have demonstrated that the SH3-SH2-SH3 domain of Vav2 is directly involved in the binding to the cytoplasmic domain of CD44 (Fig. 3*A*). In fact, the binding affinity of CD44 to the carboxyl-terminal SH3-SH2-SH3 fragment is comparable to CD44 binding to intact Vav2 (Fig. 3*B*). These findings suggest that the SH3-SH2-SH3 fragment of Vav2 is responsible for the recognition of CD44 *in vitro*. In addition, we have detected that the binding of HA to CD44v3 promotes Vav2-catalyzed Rac1 activation (Fig. 4) and tumor cell migration (Table V). Therefore, we believe that CD44v3 is both a cell membrane attachment site and an activator for Vav2 function. Clearly, these two proteins (CD44v3 and Vav2) are not only structurally linked but also functionally coupled.

Recent studies (83, 84) have demonstrated that receptor-induced formation of macromolecular signaling complexes is often mediated by molecular scaffolds and adaptors. In this regard, Vav2 is known to interact with adaptor proteins, such as Grb2 (69, 70), that mediate binding to the oncogene product $p185^{HER2}$ in transformed cells (49–52, 55). The question of whether the CD44v3-Vav2 complex is also involved in the communication with other oncogenic signaling components (*e.g.* $p185^{HER2}$ and/or Grb2) in ovarian tumor cells is addressed in this study. The HER-2/Neu (also known as ErbB-2) protooncogene encodes a 185-kDa transmembrane glycoprotein with intrinsic tyrosine activity homologous to the epidermal growth factor receptor (44, 45). Amplification/overexpression of the HER-2/Neu oncogene is often associated with human ovarian cancers and poor clinical prognosis in patients (46, 47). Previously, we have found that CD44 expression is concomitantly up-regulated with $p185^{HER2}$ in a mouse fibroblast cell line (85) and in human ovarian tumor cells (2). Up-regulation of surface CD44 in those $p185^{HER2}$-overexpressed cells results in a dramatic enhancement of HA-mediated

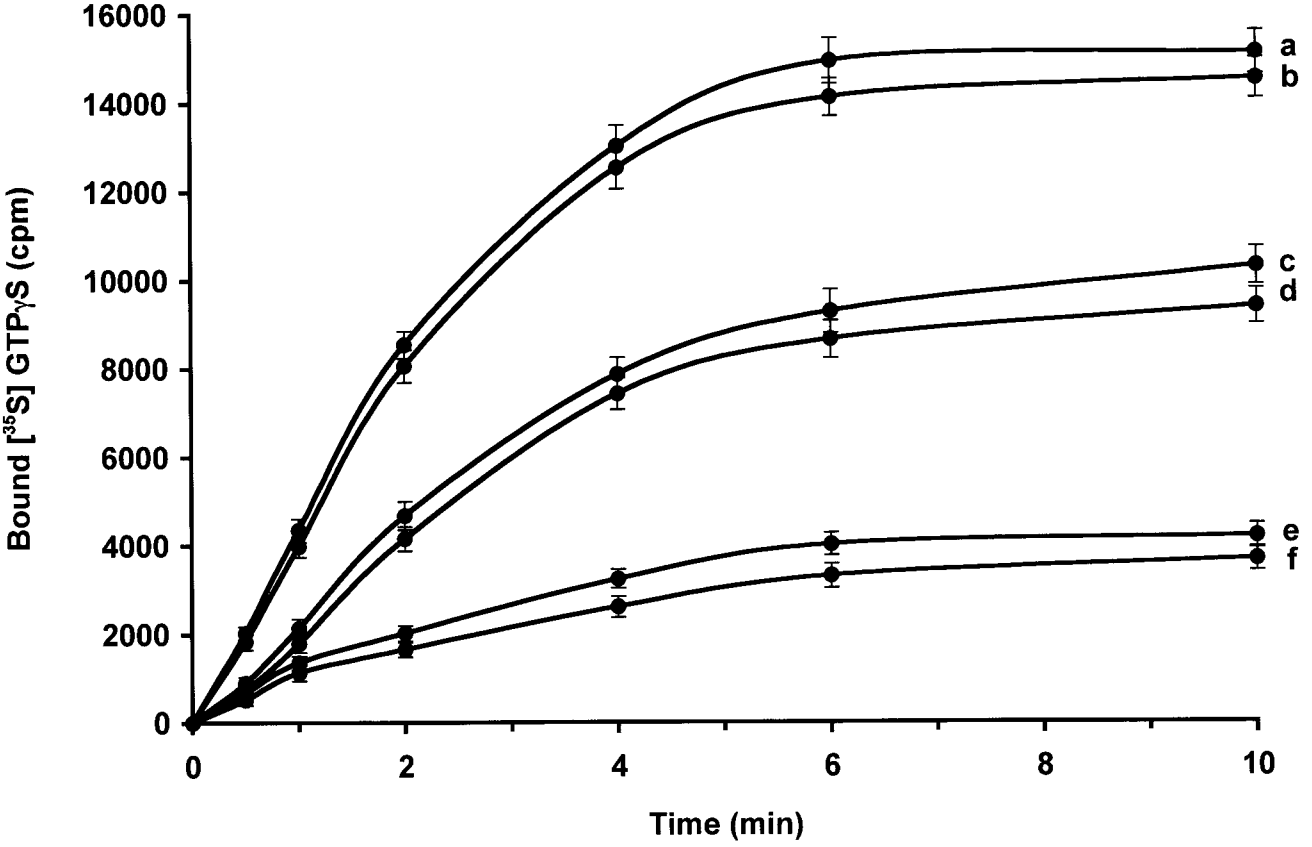

FIG. 7. **Kinetics of [^{35}S]GTPγS bound to GDP-loaded Rac1 in the presence of Vav2 isolated from SK-OV-3.ipl cells transfected with HA1-tagged ΔC-Grb2cDNA, HA1-tagged ΔN-Grb2cDNA, or vector alone.** Purified *E. coli*-derived GST-tagged Rac1 was preloaded with GDP. First, 2 pmol of Vav2 isolated from various SK-OV-3.ipl transfectants (in the presence or absence of 50 μg/ml HA) was added to the reaction buffer containing 20 mM Tris-HCl (pH 8.0), 100 mM NaCl, 10 mM $MgCl_2$, 100 μM AMP-PNP, 0.5 mg/ml bovine serum albumin, and 2.5 μM [^{35}S]GTPγS (≈1,250 Ci/mmol). Subsequently, 2.5 pmol of GDP-loaded GST-tagged Rac1 was mixed with the reaction buffer containing Vav2 and [^{35}S]GTPγS to initiate the exchange reaction at room temperature. At various time points, the reaction of each sample was terminated by adding ice-cold termination buffer as described under "Materials and Methods." The amount of [^{35}S]GTPγS bound to Vav2 or control sample (preimmune serum-conjugated Sepharose beads) in the absence of Rac1 was subtracted from the original values. Data represent an average of triplicates from 3 to 5 experiments. The S.D. was less than 5%. *Curve a,* the GDP/GTP exchange reaction on Rac1 by Vav2 isolated from vector-transfected cells treated with HA. *Curve b,* the GDP/GTP exchange reaction on Rac1 by Vav2 isolated from HA1-tagged ΔC-Grb2cDNA-transfected cells treated with HA. *Curve c,* the GDP/GTP exchange reaction on Rac1 by Vav2 isolated from vector-transfected cells without any HA treatment. *Curve d,* the GDP/GTP exchange reaction on Rac1 by Vav2 isolated from HA1-tagged ΔC-Grb2cDNA-transfected cells without any HA treatment. *Curve e,* the GDP/GTP exchange reaction on Rac1 by Vav2 isolated from HA1-tagged ΔN-Grb2cDNA-transfected cells treated with HA. *Curve f,* the GDP/GTP exchange reaction on Rac1 by Vav2 isolated from HA1-tagged ΔN-Grb2cDNA-transfected cells without any HA treatment.

cell adhesion (85) and tumor cell growth (2). In this study we have also observed that $p185^{HER2}$ is co-expressed with CD44v3 in human ovarian tumor cells (Figs. 5 and 6) and that a close association exists between CD44v3 and $p185^{HER2}$ in SK-OV-3.ipl cells (Figs. 5*B* and 6*C*). Our previous study has shown that CD44 and $p185^{HER2}$ are closely associated with each other in a complex involving interchain disulfide bonds in ovarian tumor cells (2). Several cysteine residues including 6–7 cysteine residues at the external domain, 1 Cys (aa 286) in the transmembrane region, and 1 Cys (aa 295) have been identified in the cytoplasmic domain of CD44 (86). It is likely that some of these cysteine residues of CD44 are involved in the disulfide linkage with one or more cysteine residues in $p185^{HER2}$. The question of which cysteine residues in human CD44 are directly responsible for forming disulfide linkages with $p185^{HER2}$ remains to be determined. The association of $p185^{HER2}$ with other surface molecules via disulfide linkages has also been reported previously (87). Although CD44 and $p185^{HER2}$ are physically linked via interchain disulfide bonds (2), it is also possible that these two membrane proteins can be complexed together through other linker molecules (*e.g.* Grb2).

Upon activation of the cells, HER-2/neu is phosphorylated at tyrosine residues in its intracellular domain that provides docking sites for Src homology 2 (SH2) and/or protein tyrosine binding domain-containing proteins (44, 45). One of the signaling molecules known to be recruited to the tyrosine phosphorylation sites of HER-2/neu is Grb2, which was originally identified as a growth factor receptor-bound protein (known as a mammalian homolog of *Caenorhabditis elegans* Sem5 and *Drosophila* Drk) (88–90). Grb2 is a 24-kDa adaptor protein containing an SH2 domain flanked by two SH3 domains (Fig. 6*A*). Through the SH3 domains, Grb2 is constitutively associated with Sos (named for the Sons of Sevenless gene), a 150-kDa GEF for Ras, by targeting the proline-rich motif as its carboxyl terminus (48–55). Furthermore, membrane relocalization of Sos by recruitment of the Grb2-Sos complex causes Ras activation (48–55). Ras activation, in turn, stimulates a downstream kinase cascade, the Raf-1/MEK/MAPK pathway leading to cell growth (48–54). Ras-activated MAPK (in particular, ERK1 and ERK2) also plays an important role in modulating cytoskeleton function and/or influencing cell motility (91, 92). Thus, the Ras-MAPK signaling pathways appear to be involved in the onset of multiple functions including growth and/or motility. The fact that a dominant-negative mutant of Grb2, which impairs the association of Grb2 with $p185^{HER2}$, inhibits Ras activation and induces reversal of the transformed phenotypes

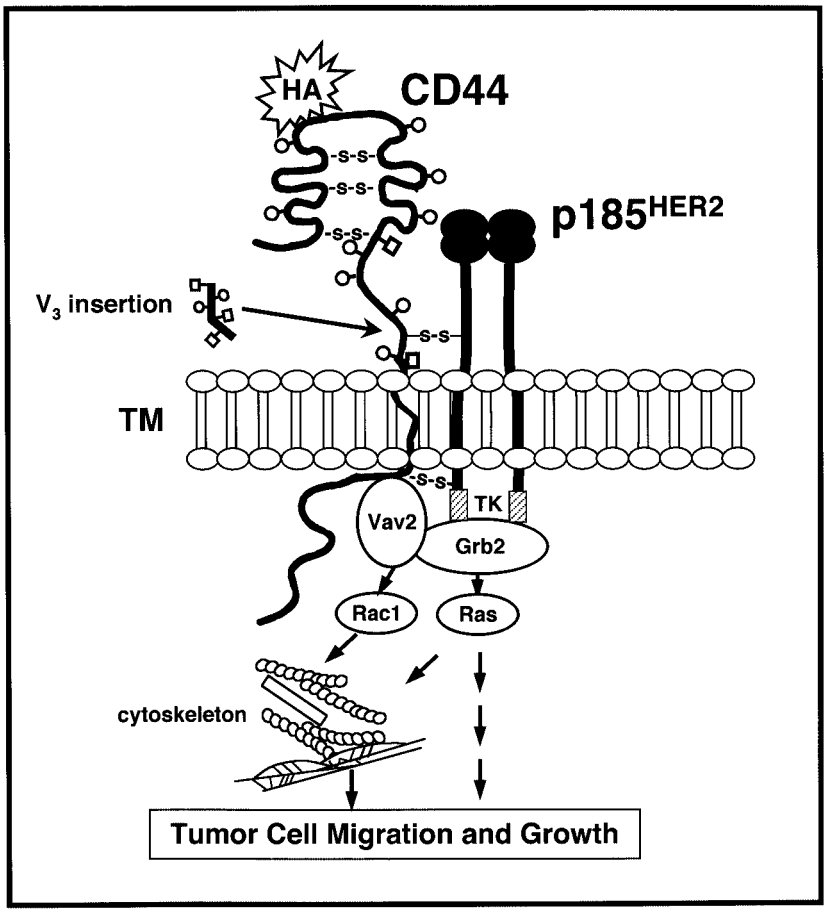

FIG. 8. **A proposed model for the interaction between CD44v3-Vav2 and Grb2-p185^{HER2} during oncogenic signaling and ovarian tumor progression.** The binding of HA to CD44v3 isoform (containing the v3 exon-encoded structure) induces CD44v3 interaction with Vav2 which, in turn, activates RhoGTPase (Rac1) signaling leading to cytoskeleton activation and tumor cell migration. HA binding to the CD44v3-p185^{HER2} complex (formed by a disulfide linkage) results in p185^{HER2} tyrosine kinase (*TK*) activation, which recruits the adaptor molecule, Grb2, into the CD44v3-p185^{HER2} complex. The ability of Grb2 (complexed with CD44v3 and p185^{HER2}) to stimulate Ras signaling, and to interact with Vav2 for Rac1 signaling, promotes the concomitant onset of tumor cell growth and migration leading to ovarian tumor progression.

caused by p185^{HER2} suggests that Grb2 is responsible for the p185^{HER2}-induced oncogenesis (55). We have now demonstrated that Grb2 is also expressed in SK-OV-3.ipl cells (Fig. 5*B*) and that it is associated with a CD44v3 and p185^{HER2}-containing signaling complex in the ovarian tumor cells (Fig. 5*B*). HA binding to CD44v3 stimulates p185^{HER2} tyrosine kinase (Fig. 5*A*) which, in turn, recruits Grb2 into the CD44v3-p185^{HER2} signaling complex (Fig. 5*B*). Grb2 has been shown to bind directly to p185^{HER2} (55). Therefore, it is possible that HA/CD44-activated p185^{HER2} is involved in the recruitment of Grb2 into the CD44v3-p185^{HER2} signaling complex (Fig. 5*B*). A number of other Ras GEFs have also been reported. For example, C3G (known as Crk SH3-binding GEF) can activate Ras in yeast via the binding of its proline-rich domain to the amino-terminal domain of the adaptor protein, Crk (93, 94). The Crk-C3G complex may thus mimic the Grb2-Sos complex and couple the oncogenic signal of the mutation-activated p185^{HER2} to Ras (93, 94). Therefore, we cannot rule out the possibility that Crk-C3G complex is also involved in Ras activation during HA-stimulated CD44v3/p185^{HER2} signaling events. Identification of the immediate upstream activator(s) for Ras during CD44v3/p185^{HER2}-activated oncogenic events is currently under investigation in our laboratory.

It has been reported that Grb2 may have other cellular functions in addition to linking receptor tyrosine kinases to the Ras signaling pathway. Microinjection studies with anti-Grb2 antibodies in rat kidney cells suggest that Grb2 may play a role in signaling from receptor tyrosine kinase to the small GTP-binding protein Rac (93). Also, the Grb2-SH3 domains have been shown to bind several proteins besides Sos1, including Vav (69, 70), p85 (94), Sos2, and other proteins (p228, p140, p55, and p28) (95–98). The multiple Grb2-SH3 domain interactions may mediate novel cellular functions of this adaptor protein. In this study we have observed that endogenous Grb2 is complexed with CD44v3-Vav2 and p185^{HER2} in a signaling complex and that HA treatment induces recruitment of Grb2 (together with p185^{HER2}) into CD44v3-containing multimolecular complexes (Fig. 5*B*) leading to the co-activation of Rac1 (Figs. 4 and 7) and Ras signaling (Table III) and ovarian tumor cell growth (Table IV) and migration (Table V). These observations strongly suggest that Grb2 not only plays an important role in receptor tyrosine kinase (p185^{HER2})-mediated Ras signaling pathway (Table III) (15, 16, 17, 18), but also participates in CD44v3-Vav2-mediated Rac1 signaling pathway (Figs. 4 and 7). Although Grb2 is known to bind to Vav2 (69, 70), the important question of whether Grb2 interacts with CD44 directly awaits further investigation. The fact that transfection of SK-OV-3.ipl cells with ΔN-Grb2cDNA (but not ΔC-Grb2cDNA) not only abolishes Grb2 association with CD44v3-Vav2 complexes (Fig. 6), but also inhibits its binding to p185^{HER2} (Fig. 6), suggests that the amino-terminal SH3 domain of Grb2 (not the carboxyl-terminal SH3 domain of Grb2) is directly involved in the assembly of these diverse signaling molecules containing CD44v3-Vav2 and p185^{HER2}. Most importantly, overexpression of the dominant-negative mutant protein, ΔN-Grb2 (and to a lesser extent the ΔC-Grb2), inhibits HA-dependent tumor cell behaviors (*e.g.* Rac1 (Fig. 7), Ras activation (Table III), tumor cell growth (Table IV), and migration (Table V)). These observations further support the conclusion that interfering with the interaction between these diverse signaling molecules (containing CD44v3-Vav2 and p185^{HER2} and the endogenous Grb2) by ΔN-Grb2 impairs oncogenic signaling (*e.g.* Rac1 and Ras activation) and ovarian tumor cell behaviors (*e.g.* tumor cell migration and growth). Our results are consistent with previous

findings indicating that dominant-negative mutants of Grb2 lacking the amino-(ΔN-Grb2) or carboxyl-(ΔC-Grb2) terminal SH3 domains can reverse p185-activated cell transformation (55).

In summary, we would like to propose that CD44v3-Vav2 interaction with Grb2-p185^{HER2} forms an important signaling complex that plays a pivotal role in promoting direct cross-talk between the Rac1 signaling pathway and the Ras signaling pathway leading to the concomitant onset of ovarian tumor cell migration and growth during ovarian cancer progression (Fig. 8). Under physiologic conditions, hyaluronan often exists as a high molecule polymer ($>10^6$ daltons). However, under the condition of tumorigenesis, generation of hyaluronan fragments may occur. Both HA and certain size HA fragments (3–25 disaccharide units) have been found to promote CD44-specific cell proliferation (5) and interleukin-8 gene expression (76). The question of whether certain small size HA fragments are capable of promoting the same CD44v3-Vav2 and Grb2-p185^{HER2} oncogenic signaling and ovarian tumor cell migration/growth as the native large molecular weight hyaluronan used in this study is currently undergoing investigation in our laboratory.

Acknowledgment—We gratefully acknowledge Dr. Gerard J. Bourguignon for assistance in the preparation of this paper.

REFERENCES

1. Screaton, G. R., Bell, M. V., Jackson, D. G., Cornelis, F. B., Gerth, U., and Bell, J. I. (1992) *Proc. Natl. Acad. Sci. U. S. A.* **89,** 12160–12164
2. Bourguignon, L. Y. W., Zhu, H. B., Chu, A., Zhang, L., and Hung, M. C. (1997) *J. Biol. Chem.* **272,** 27913–27918
3. Lokeshwar, V. B., and Bourguignon, L. Y. W. (1991) *J. Biol. Chem.* **266,** 17983–17989
4. Bourguignon, L. Y. W., Lokeshwar, V. B., He, J., Chen, X., and Bourguignon, G. J. (1992) *Mol. Cell. Biol.* **12,** 4464–4471
5. Lokeshwar, V. B., Iida, N., and Bourguignon, L. Y. W. (1996) *J. Biol. Chem.* **271,** 23853–23864
6. Underhill, C. (1992) *J. Cell Sci.* **103,** 293–298
7. Liao, H. X., Lee, D. M., Levesque, M. C., and Haynes, B. F. (1995) *J. Immunol.* **155,** 3938–3945
8. Yang, B., Yang, B. L., Savani, R. C., and Turley, E. A. (1994) *EMBO J.* **13,** 286–296
9. Lokeshwar, V. B., Fregien, N., and Bourguignon, L. Y. W. (1994) *J. Cell Biol.* **126,** 1099–1109
10. Bourguignon, L. Y. W. (1996) *Curr. Top. Membr.* **43,** 293–312
11. Bourguignon, L. Y. W., Zhu, D., and Zhu, H. (1998) *Front. Biosci.* **3,** 637–649
12. Zhu, D., and L. Y. W. Bourguignon. (1998) *Cell Motil. Cytoskeleton* **39,** 209–222
13. Zhu, D., and Bourguignon, L. Y. W. (2000) *J. Cell. Physiol.* **183,** 182–195
14. Bretscher, A. (1999) *Curr. Opin. Cell Biol.* **11,** 109–116
15. Bourguignon, L. Y. W., Zhu, H., Shao, L., Zhu, D., and Chen, Y. W. (1999) *Cell Motil. Cytoskeleton* **43,** 269–287
16. Bourguignon, L. Y. W., Zhu, H., Shao, L., and Chen, Y. W. (2000) *J. Cell Biol.* **150,** 177–191
17. Bourguignon, L. Y. W., Zhu, H., Shao, L., and Chen, Y. W. (2000) *J. Biol. Chem.* **275,** 1829–1838
18. Oliferenko, S., Kaverina, I., Small, J. V., and Huber, L. A. (2000) *J. Cell Biol.* **148,** 1159–1164
19. Bourguignon, L. Y. W., Zhu, H., Shao, L., and Chen, Y. W. (2001) *J. Biol. Chem.* **276,** 7327–7336
20. Green, S. J., Tarone, G., and Underhill, C. B. (1988) *Exp. Cell Res.* **178,** 224–232
21. West, D. C., and Kumar, S. (1989) *Exp. Cell Res.* **183,** 179–196
22. Turley, E. A., Austen, L., Vandeligt, K., and Clary, C. (1991) *J. Cell Biol.* **112,** 1041–1047
23. Rooney, P., Kumar, S., and Wang, M. (1995) *Int. J. Cancer* **60,** 632–636
24. Gardner, M. J., Jones, L. M. H., Catterall, J. B., and Turner, G. A. (1995) *Cancer Lett.* **91,** 229–234
25. Cerione, R. A., and Zheng, Y. (1996) *Curr. Opin. Cell Biol.* **8,** 216–222
26. Whitehead, I. P., Campbell, S., Rossman, K. L., and Der, C. J. (1997) *Biochim. Biophys. Acta* **1332,** F1–F-23
27. Schuebel, K. E., Movilla, N., Rosa, J. L., and Bustelo, X. R. (1998) *EMBO J.* **17,** 6608–6621
28. Katzav, S., Martin-Zanca, D., and Barbacid, M. (1989) *EMBO J.* **8,** 2283–2290
29. Bustelo, X. R. (2000) *Mol. Cell. Biol.* **20,** 1461–1477
30. Schuebel, K. E., Bustelo, X. R., Nielsen, D. A., Song, B. J., Barbacid, M., Goldman, D., and Lee, I. J. (1996) *Oncogene* **13,** 363–371
31. Coppola, J., Bryant, S., Koda, T., Conway, D., and Barbacid, M. (1991) *Cell Growth Differ.* **2,** 95–105
32. Adams, J. M., Houston, H., Allen, J., Lints, T., and Harvey, R. (1992) *Oncogene* **7,** 611–618
33. Boguski, M. S., and McCormick, F. (1993) *Nature* **366,** 643–654
34. Musacchio, A., Gibson, T., Rice, P., Thompson, J., and Saraste, M. (1993) *Trends Biochem. Sci.* **18,** 343–348
35. Bustelo, X. R., and Barbacid, M. (1992) *Science* **256,** 1196–1199
36. Margolis, B., Hu, P., Katzav, S., Li, W., Oliver, J. M., Ullrich, A., Weiss, A., and Schlessinger, J. (1992) *Nature* **356,** 71–74
37. Han, J., Das, B., Wei, W., Van Aelst, L., Mosteller, R. D., Khosravi-Far, R., Westwick, J. K., Der, C. J., and Broek, D. (1997) *Mol. Cell. Biol.* **17,** 1346–1353
38. Crespo, P., Schuebel, K. E., Ostrom, A. A., Gutkind, J. S., and Bustelo, X. R. (1997) *Nature* **385,** 169–172
39. Olson, M. F., Pasteris, N. G., Gorski, J. L., and Hall, A. (1996) *Curr. Biol.* **6,** 1628–1633
40. Abe, K., Rossman, K. L., Liu, B., Ritola, K. D., Chiang, D., Campbell, S. L., Burridge, K., and Der, C. J. (2000) *J. Biol. Chem.* **275,** 10141–10149
41. Shaw, G. (1996) *BioEssays* **18,** 35–46
42. Hemmings, B. A. (1997) *Science* **275,** 1899
43. Hall, A. (1998) *Science* **279,** 509–514
44. Bargmann, C. I., Hung, M. C., and Weinberg, R. A. (1986) *Cell* **45,** 649–657
45. Pele, E., and Yarden, Y. (1993) *BioEssays* **15,** 815–823
46. Berchuck, A., Kamel, A., Whitaker, R., Kerns, B., Olt, G., Kinney, R., Soper, J. T., Dodge, R., Clarke-Pearson, D. L., Marks, P., McKenzie, P., Yin, S., and Bast, J. R. C. (1990) *Cancer Res.* **50,** 4087–4091
47. Hung, M. C., Zhang, X., Yen, D.-H., Zhang, H.-Z., He, G.-P., Zhang, T.-Q., and Shi, D. R. (1992) *Cancer Lett.* **61,** 95–103
48. Slamon, D. J., Williams, G., Jones, L. A., Holt, J. A., Wong, S. G., Keith, D. E., Levin, W. J., Stuart, S. G., Udove, J. Ullrich, A., and Press, M. F. (1989) *Science* **244,** 707–712
49. Gale, N. W., Kaplan, S., Lowenstein, E. J., Schlessinger, J., and Bar-Sagi, D. (1993) *Nature* **363,** 88–92
50. Egan, S. E., Giddings, B. W., Brooks, M. W., Buday, L., Sizeland, A. M., and Weinberg, R. A. (1993) *Nature* **363,** 45–51
51. Buday, L., and Downward, J. (1993) *Cell* **73,** 611–620
52. Rozakis-Adcock, M., Fernley, R., Wade, J., Pawson, T., and Bowtell, D. (1993) *Nature* **363,** 83–85
53. Li, N., Batzer, A., Daly, R., Yajnik, V., Skolnik, E., Chardin, P., Bar-Sagi, D., Margolis, B., and Schlessinger, J. (1993) *Nature* **363,** 85–88
54. Chardin, P., Camonis, J. H., Gale, N. W., Van Aelst, L., Schlessinger, J., Wigler, M. H., and Bar-Sagi, D. (1993) *Science* **260,** 1338–1343
55. Xie, Y., Pendergast, A. M., and Hung, M. C. (1995) *J. Biol. Chem.* **270,** 30717–30724
56. Bourguignon, L. Y. W., Gunja-Smith, Z., Iida, N., Zhu, H. B., Young, L. J. T., Muller, W. J., and Cardiff, R. D. (1998) *J. Cell. Physiol.* **176,** 206–215
57. Iida, N., and Bourguignon, L. Y. W. (1995) *J. Cell. Physiol.* **162,** 127–133
58. Chu, G., Hayakawa, H., and Berg, P. (1987) *Nucleic Acids Res.* **15,** 1311–1326
59. Zhang, Y., Hart, M. J., and Cerione, R. A. (1995) *Method Enzymol.* **256,** 77–84
60. Zhang, K., Papageorge, A. G., and Lowy, D. R. (1992) *Science* **257,** 671–674
61. Merzak, A., Koochekpour, S., and Pilkington, G. J. (1994) *Cancer Res.* **54,** 3988–3992
62. Bennett, K., Jackson, D. G., Simon, J. C., Tanczos, E., Peach, R., Modrell, B., Stamenkovic, I., Plowman, G., and Aruffo, A. (1995) *J. Cell Biol.* **128,** 687–698
63. Dvorak, H. F., Brown, L. F., Detmar, M., and Dvorak, A. M. (1995) *Am. J. Pathol.* **146,** 1029–1039
64. Hobert, O., Jallal, B., Schlessinger, J., and Ullrich, M. A. (1994) *J. Biol. Chem.* **269,** 20225–20228
65. Romero, F., Germani, A., Puvion, E., Camonis, J., Varin-Blank, N., Gisselbrecht, S., and Fischer, S. (1998) *J. Biol. Chem.* **273,** 5923–5931
66. Romero, F., Dargemont, C., Pozo, F., Reeves, W. H., Camonis, J., Gisselbrecht, S., and Fisher, S. (1996) *Mol. Cell. Biol.* **16,** 37–44
67. Hobert, O., Schilling, J. W., Beckerle, M. C., Ullrich, A., and Jallal, B. (1996) *Oncogene* **12,** 1577–1581
68. Liu, B. P., and Burridge, K. (2000) *Mol. Cell. Biol.* **20,** 7160–7169
69. Ye, Z. S., and Baltimore, D. (1994) *Proc. Natl. Acad. Sci. U. S. A.* **91,** 12629–12633
70. Ramos-Morales, F., Romero, F., Schweighoffer, F., Bismuth, G., Camonis, J., Tortolero, M., and Fischer, S. (1995) *Oncogene* **11,** 1665–1669
71. Cannistra, S. A., Kansas, G. S., Niloff, J., DeFranzo, B., Kim, Y., and Ottensmeier, C. (1993) *Cancer Res.* **53,** 3830–3838
72. Cannistra, S. A., DeFranzo, B., Niloff, J., and Ottensmeier, C. (1995) *Clin. Cancer Res.* **1,** 333–342
73. Bourguignon, L. Y. W., Kalomiris, E. L., and Lokeshwar, V. B. (1991) *J. Biol. Chem.* **266,** 11761–11765
74. Lokeshwar, V. B., and Bourguignon, L. Y. W. (1992) *J. Biol. Chem.* **267,** 22073–22078
75. Kalomiris, E. L., and Bourguignon, L. Y. W. (1989) *J. Biol. Chem.* **264,** 8113–8119
76. Bourguignon, L. Y. W. (2001) *J. Mammary Gland Biol. & Neoplasia* **6,** 287–297
77. Bourguignon, L. Y. W., Lokeshwar, V. B., Chen, X., and Kerrick, G. L. (1993) *J. Immunol.* **151,** 6634–6644
78. Ridley, A. J., Paterson, C. L., Johnston, C. L., Diekmann, D., and Hall, A. (1992) *Cell* **70,** 401–410
79. Nobes, C. D., and Hall, A. (1995) *Cell* **81,** 53–62
80. Coso, O. A., Chiariello, M., Yu, J. C., Teramoto, H., Crespo, P., Xu, N. G., Miki, T., and Gutkind, J. S. (1995) *Cell* **81,** 1137–1146
81. Minden, A., Lin, A. N., Claret, F. X., Abo, A., and Karin, M. (1995) *Cell* **81,** 1147–1157
82. Arudchandran, R., Brown, M. J., Peirce, M. J., Song, J. S., Zhang, J., Siraganian, R. P., Blank, U., and Rivera, J. (2000) *J. Exp. Med.* **191,** 47–59
83. Rudd, C. E. (1999) *Cell* **96,** 5–8
84. Cantrell, D. (1988) *Trends Cell Biol.* **8,** 180–182
85. Zhu, D., and Bourguignon, L. Y. W. (1996) *Oncogene* **12,** 2309–2314
86. Liu, D., and Sy, M. S. (1996) *J. Exp. Med.* **183,** 1987–1994
87. Adelsman, M. A., Huntley, B. K., and Maihle, N. J. (1996) *J. Virol.* **70,** 2533–2544

88. Lowenstein, E. J., Daly, R. J., Batzer, A. G., Li, W., Margolis, B., Lammers, R., Ullrich, A., Skolnik, E. Y., Bar-Sagi, D., and Schlessinger, J. (1993) *Cell* **70,** 431–442
89. Simon, M. A., Dodson, G. S., and Rubin, G. M. (1993) *Cell* **73,** 169–177
90. Olivier, J. P., Raabe, T., Henkemeyer, M., Dickson, B., Mbamalu, G., Margolis, B., Schlessinger, J., Hafen, E., and Pawson, T. (1993) *Cell* **73,** 179–191
91. Klemke, R. L., Cai, S., Giannini, A. L., Gallagher, P. J., de Lanerolle, P., and Cheresh, D. (1997) *J. Cell Biol.* **137,** 481–492
92. Krueger, J. S., Keshamouni, V. G., Atanaskova, N., and Reddy, K. B. (2001) *Oncogene* **20,** 4209–4218
93. Tanaka, S., Morishita, T., Hashimoto, Y., Hattori, S., Nakamura, S., Shibuya, K., Matuoka, K., Takenawa, T., Kurata, T., Nagashima, K., and Matsuda, M. (1994) *Proc. Natl. Acad. Sci. U. S. A.* **91,** 3443–3447
94. Matsuda, M., Hashimoto, Y., Muroya, N., Hasegawa, H., Kurata, T., Tanaka, S., Nakamura, S., and Hattori, S. (1994) *Mol. Cell. Biol.* **14,** 495–5500
95. Matuoka, K., Shibasaki, F., Shibata, M., and Takenawa, T. (1993) *EMBO J.* **12,** 3467–3473
96. Wang, J., Auger, K. R., Jarvis, L., Shi, Y., and Roberts, T. M. (1995) *J. Biol. Chem.* **270,** 12774–12780
97. Yang, S. S., Van Aelst, L., and Bar-Sagi, D. J. (1995) *J. Biol. Chem.* **270,** 18212–18215
98. Sastry, L., Cao, T., and King, C. R. (1997) *Int. J. Cancer* **70,** 208–213